NOVIA
UNIVERSITY OF APPLIED SCIENCES

Active Engine Control Based on Gas Quality

Kristian Haka

Degree Thesis for Master of Engineering

Degree Programme in Automation Technology

Vaasa 2019

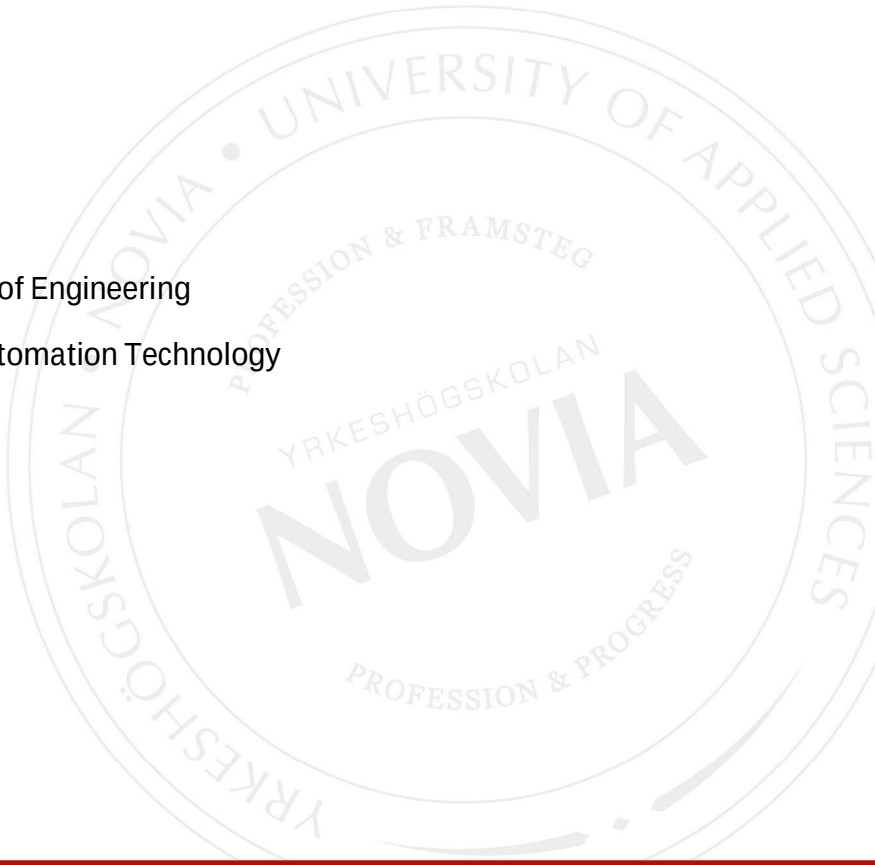

MASTER'S THESIS

Author: Kristian Haka
Degree Programme: Automation Technology, Vaasa
Supervisor: Ray Pörn

Title: Active Engine Control Based on Gas Quality

Date: May 14, 2019 Number of pages: 61 Appendices: 2

Abstract

The usage of gaseous fuels in internal combustion engines for transportation and power generation is continuously growing. The quality of gaseous fuels is often defined as their knock resistance, where the methane number is the most important property. Variations in gaseous fuel composition present several challenges for engine operation. They affect the combustion properties and can even result in engine knock. In order to assure reliable operation and prevent engine knock, it might be necessary to restrict the power output from the engine depending on the gaseous fuel quality.

The objective of this thesis was to design and implement a controller that is determining maximum allowed power output based on the gaseous fuel quality. The implementation was primarily done into a PLC system, but it can easily also be implemented to other control systems as the design is model based. A study was also done to investigate other possible engine control applications utilizing the gas quality measurement technology. The controller design work includes and addresses e.g. signal filtering, screening of other control functions making sure that they are not interfering, and design of controller dynamics based on the response time of the measurement equipment.

The functionality of the controller is presented, and correct function was confirmed by a simulation with real measurement data from an operating power plant. Finally, the future utilization of the controller and gas quality measurement technology is presented.

Language: English Key words: gas quality, methane number, gas engine, knock, engine control, model-based design

---

OPINNÄYTETYÖ

Tekijä: Kristian Haka
Koulutus ja paikkakunta: Automation Technology, Vaasa
Ohjaaja: Ray Pörn

Nimike: Adaptiivinen moottorinohjaus kaasun laadun perusteella

---

Päivämäärä: 14.5.2019 Sivumäärä: 61 Liitteet: 2

Tiivistelmä

Kaasumuotoisen polttoaineen käyttö kuljetusajonevojen ja energiantuotannon polttomoottoreissa kasvaa koko ajan. Kaasumaisten polttoaineiden laatu määritellään usein niiden nakutuskestävyyden mukaan. Näiden polttoaineiden tärkein ominaisuus on metaaniluku. Kaasumaisen polttoaineen koostumusvaihtelut aiheuttavat useita haasteita moottorin toiminnalle. Kaasumaisen polttoaineen koostumusvaihtelut vaikuttavat palamisominaisuuksiin ja voi jopa johtaa moottorinakutukseen. Taatakseen luotettavan toiminnan ja moottorinakutuksen estämiseksi, on moottorin tehoa mahdollisesti rajoitettava kaasumaisen polttoaineen laadun mukaan.

Tämän opinnäytetyön tavoitteena oli suunnitella ja toteuttaa säädin, joka määrittää suurimman sallitun moottoritehon kaasumaisen polttoaineen laadun perusteella. Toteutus tehtiin ensisijaisesti ohjelmoitavassa ohjausjärjestelmässä (PLC). Tämä mallipohjainen suunnittelu mahdollistaa jatkossa toteutuksen myös muille ohjausjärjestelmille. Tutkimuksessa haluttiin selvittää, onko muita mahdollisia moottorinhallintaan vaikuttavia sovelluksia, jotka perustuvat kaasun laadun mittausteknologiaan. Säätimen suunnittelutyö käsittelee mm. signaalin suodatuksen, yhtäaikaisen käytön muiden moottoriohjauslaitteiden kanssa, ja säätimen dynamiikan suunnittelu perustuen mittauslaitteiston vastausaikaan.

Työssä esitetään säätimen toiminnallisuus, ja sen oikeanlainen toiminta vahvistetaan simuloinnilla. Simuloinnissa käytetiin todellisia mittaustietoja toimivalta voimalaitokselta. Lopuksi esitellään säätimen ja kaasun laadun mittaustekniikan tulevaa käyttöä.

Kieli: englanti Avainsanat: kaasun laatu, metaaniluku, kaasumoottori, nakutus, moottorinohjaus, mallipohjainen suunnittelu

---

EXAMENSARBETE

Författare: Kristian Haka
Utbildning och ort: Automation Technology, Vasa
Handledare: Ray Pörn

Titel: Adaptiv motorkontroll baserad på gaskvalitet

Datum: 14.5.2019 Sidantal: 61 Bilagor: 2

Abstrakt

Användningen av gasformiga bränslen i förbränningsmotorer för transport och energiproduktion ökar ständigt. Kvaliteten hos gasformiga bränslen bestäms vanligtvis av deras knackmotstånd, av vilka metantalet är den viktigaste egenskapen. Variationen i sammansättningen hos det gasformiga bränslet utgör ett antal utmaningar för motorns drift. Det inverkar på förbränningsegenskaper och kan även leda till motorknack. För att trygga en pålitlig drift samt förhindra motorknack kan det vara nödvändigt att begränsa motorns effekt baserad på kvaliteten på det gasformiga bränslet.

Målet med detta examensarbete var att planera och förverkliga en regulator som bestämmer högsta tillåtna motoreffekt, vilken fastställs av kvaliteten på det gasformiga bränslet. Genomförandet gjordes i första hand i ett programmerbart styrsystem (PLC), men eftersom framställningen gjordes som en modellbaserad utformning kan den även enkelt förverkligas i andra styrsystem. En undersökning genomfördes också för att undersöka andra möjliga tillämpningar av motorkontroll som baseras på gaskvalitetsmätningsteknologin. Planeringsarbetet av regulatorn behandlar bland annat signalfiltrering, undersökning av andra motorkontrollfunktioner för att bekräfta att de inte påverkar varandra samt planering av regulatorns dynamik baserad på mätutrustningens svarstid.

Funktionaliteten hos regulatorn presenteras, och korrekt funktion verifieras med en simulering som använder sig av verklig mätdata från ett kraftverk i drift. Slutligen presenteras framtida tillämpningar av regulatorn och gaskvalitetsmätningsteknologin.

Språk: engelska Nyckelord: gaskvalitet, metantal, gasmotor, knack, motorstyrning, modellbaserad framställning

---

Table of contents

ACKNOWLEDGEMENTS / PREFACE

This thesis work was made as research and development project for Wärtsilä Finland Oy. I would first of all like to thank everyone at Wärtsilä who have been part of this project and providing support to make this a success.

I want to take the opportunity and thank my supervisor Mr. Ray Pörn for his support and valuable guidance. I would also like to express my sincere gratitude to Staffan Nysand, Kristian Blomqvist, Kaj Portin and Dennis Högberg, they have been acting as a support team and they have provided support and guidance during the entire duration of this thesis.

Vaasa, May 14, 2019

Kristian Haka

LIST OF SYMBOLS AND ABBREVIATIONS

λ	Lambda, relative air to fuel ratio
α	Filter smoothing factor
AFR	Air to fuel ratio
BC	Bottom dead centre
$BMEP$	Break mean effective pressure
CHP	Combined heat and power
CH_4	Methane
C_2H_4	Ethylene
C_2H_6	Ethene
C_3H_4	Propene
C_3H_8	Propane
CO_2	Carbon dioxide
D	Cylinder bore
DF	Dual fuel
ECU	Engine control unit
EGR	Exhaust gas re-circulation
FBD	Function block diagram
$FMEP$	Friction mean effective pressure
G_s	Specific gravity
H_2	Hydrogen
H_2S	Hydrogen sulfide
HC	Hydrocarbon
h_d	Cylinder stroke length
HHV	Higher heating value
Hz	Hertz
$IMEP$	Indicated mean effective pressure
IEC	International electrotechnical commission
IL	Instruction list
I_W	Gross Wobbe index
$I_{W(net)}$	Net Wobbe index
K_{GAS}	Gas pressure derating factor
K_{KNOCK}	Knock derating factor

K_{TC}	Turbocharger derating factor
kW	Kilowatt
LD	Ladder diagram
LHV	Lower heating value
LNG	Liquefied natural gas
LPG	Liquid petroleum gas
LPM	Litres per minute
$\dot{m}_a$	Air mass flow
$\dot{m}_f$	Fuel mass flow
m	Mass
mm	Millimetre
M	Molecular weight
MEP	Mean effective pressure
MN	Methane number
n	Number of moles
n	Number of cylinders
$n - C_4H_{10}$	n-Butane
N_2	Nitrogen
N_e	Number of revolutions per second
N_r	Number of crank revolutions per power stroke
NO_x	Nitrogen oxide
P	Pressure
PAC	Programmable automation controller
P_e	Engine power
PKI	Propane knock index
PLC	Programmable logic controller
Q_M	Mass flow
Q_V	Volume flow
R	Gas constant
RCM	Rapid compression machine
SFC	Sequential function chart
SG	Spark-ignition gas
ST	Structured text
T	Temperature

TC	Top dead centre
V	Volume
V_c	Clearance volume
$V_{C(net)}$	Net calorific value (LHV)
V_C	Gross calorific value (HHV)
V_d	Swept volume
WI	Wobbe index
WKI	Wärtsilä knock index
WMN	Wärtsilä methane number

LIST OF FIGURES

Figure Page

LIST OF TABLES

LIST OF CODE EXAMPLES

1 Introduction

There is a growing interest in using gaseous fuels which give both environmental benefits and fuel cost savings compared to liquid fuels. This will lead to a growing gas market and that will result in a larger diversity between different fuels. This increase in different gaseous fuels results in a larger variation in the chemical composition of the gas mixture and this will affect combustion properties. Variations in gaseous fuel composition present several challenges for engine operation and engines can be sensitive to variations in fuel composition. It is important regardless of what gaseous fuel is used that the engine can be operated reliable, safely and with high efficiency.

Quality of gaseous fuels is often defined as their knock resistance. This is because engine knock increases fuel consumption and pollutant emissions, but it can also physically damage the engine. Continuous monitoring of the gas quality is becoming a necessity, especially for power plants with engines that are directly connected to a gas pipeline. This enables that the engines can be controlled accordingly by continuously monitoring the gas quality in the incoming gas pipeline to the power plant.

The main objective of this thesis is to design and implement a controller that is determining the maximum allowed power output based on gas quality, this controller will be referred as the MN_derating controller. This controller will enable the engine to operate reliable and safely irrespective of changes in the incoming fuel quality. The implementation is done in a PLC system and the scope of work includes design and testing of this controller. The response time of the gas quality measurement equipment is also being investigated, since the controller dynamics are designed based on the response time.

The second part of this thesis deals with research on other possible control applications utilizing the gas quality measurement technology. By using this technology, the control of the engine can be optimized, so that the engine can be operated optimally and in the most efficient way using the available gas.

2 The internal combustion engine

This chapter will cover the basics in both the operating principle and combustion process of an internal combustion engine. The quality and the composition of the fuel have great effect on the combustion process and therefore it is useful to have knowledge of both the combustion process and effect of different fuels. In this thesis work, the focus is on four-stroke Otto engines operating with gaseous fuel.

2.1 Internal combustion engine fundamentals

A four-stroke internal combustion engine, irrespective if it uses spark ignition or compression ignition, operates in a four-stroke cycle. This four-stroke cycle includes the intake stroke, compression stroke, power stroke and exhaust stroke (Fallah & Khajepour & Goodarzi 2016, pp. 5-7). These four strokes are visualised in the following figure.

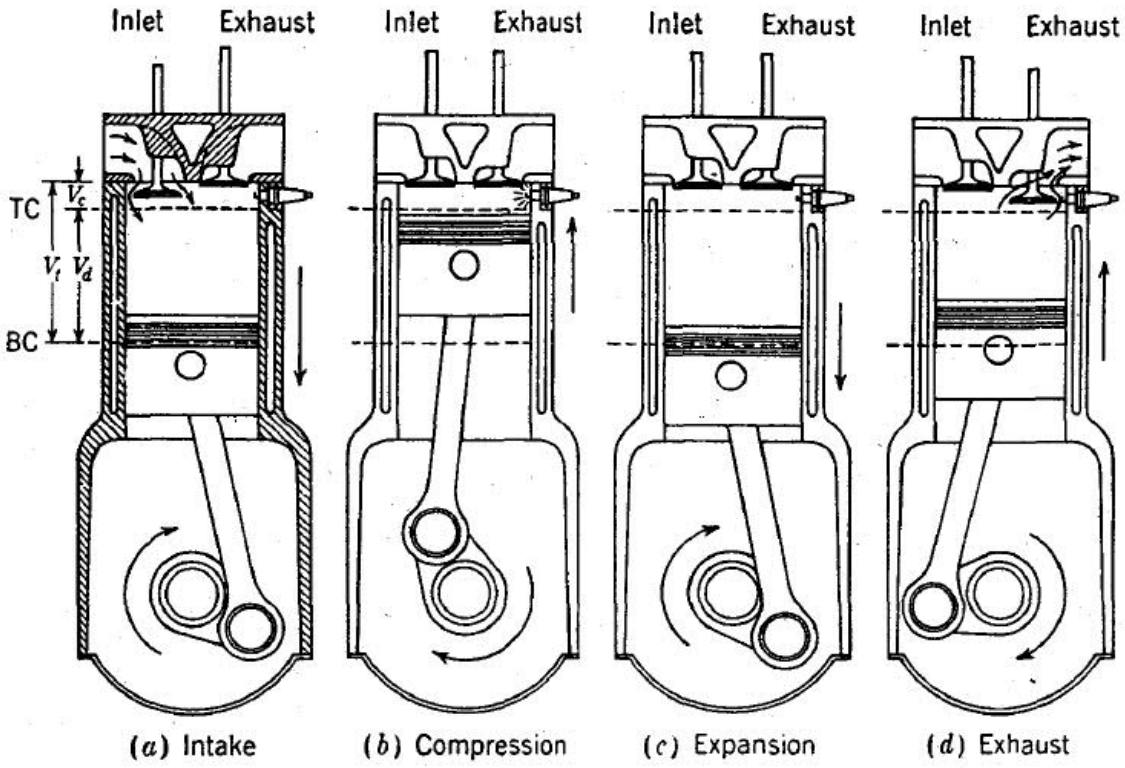

Figure 1. The operating cycle of a four stroke Otto engine (Heywood 1988, p. 10).

In the intake stroke the piston travels from top dead centre (TC) to bottom dead centre (BC) with the intake valve open and the exhaust valve closed. This creates a vacuum inside the cylinder and causes the air-fuel mixture to be sucked in. Air and fuel are pre-mixed in the intake manifold in an Otto engine (Pulkrabek 2004, pp. 25-28).

The compression stroke starts when the piston reaches BC and the intake valve closes and the piston travels back towards TC with all valves closed. This compresses the air-fuel mixture, raising both the pressure and the temperature inside the combustion chamber. Near the end of the compression stroke the gas mixture is ignited by e.g. a spark plug and the combustion process is initiated. This increases the pressure and temperature rapidly inside the combustion chamber (Pulkrabek 2004, pp. 25-28).

In the expansion stroke or also called power stroke, the high pressure created by the combustion process pushes the piston down from TC to BC. As the piston travels from TC to BC the volume inside the cylinder is increased, causing the pressure and temperature to drop and when the piston is close to BC the exhaust valve opens letting the exhaust gases out, which makes the pressure drop further. This is the stroke which produces the work and forcing the crank to rotate (Pulkrabek 2004, pp. 25-28).

In the exhaust stroke the exhaust valve remains open and the remaining gases in the cylinder are pushed out as the piston starts moving upwards again. The inlet valve opens when the piston approaches TC and just after TC the exhaust valve closes. This is the end for one operating cycle and the next operating cycle starts all over again with the intake stroke (Pulkrabek 2004, pp. 25-28).

2.2 Wärtsilä gas-fired internal combustion engines

Wärtsilä is currently manufacturing two types of gas-fired internal combustion engines in various cylinder volumes and configurations. Wärtsilä SG-series is a spark ignited gas-fired internal combustion engine, while the DF-series uses compression ignition and can be operated with both gaseous and liquid fuels. The difference in operating principle between these two types is explained in the following chapters.

2.2.1 Wärtsilä SG-series

SG-series engines are pure gas engines and work by the Otto principle and lean-burn process. These engines use a spark plug located in a pre-chamber as ignition source. The pre-chamber contains a richer air-fuel mixture that is more easily ignitable, than the lean air-fuel mixture in the main combustion chamber. The operating principle of SG-series engines is illustrated in the following figure.

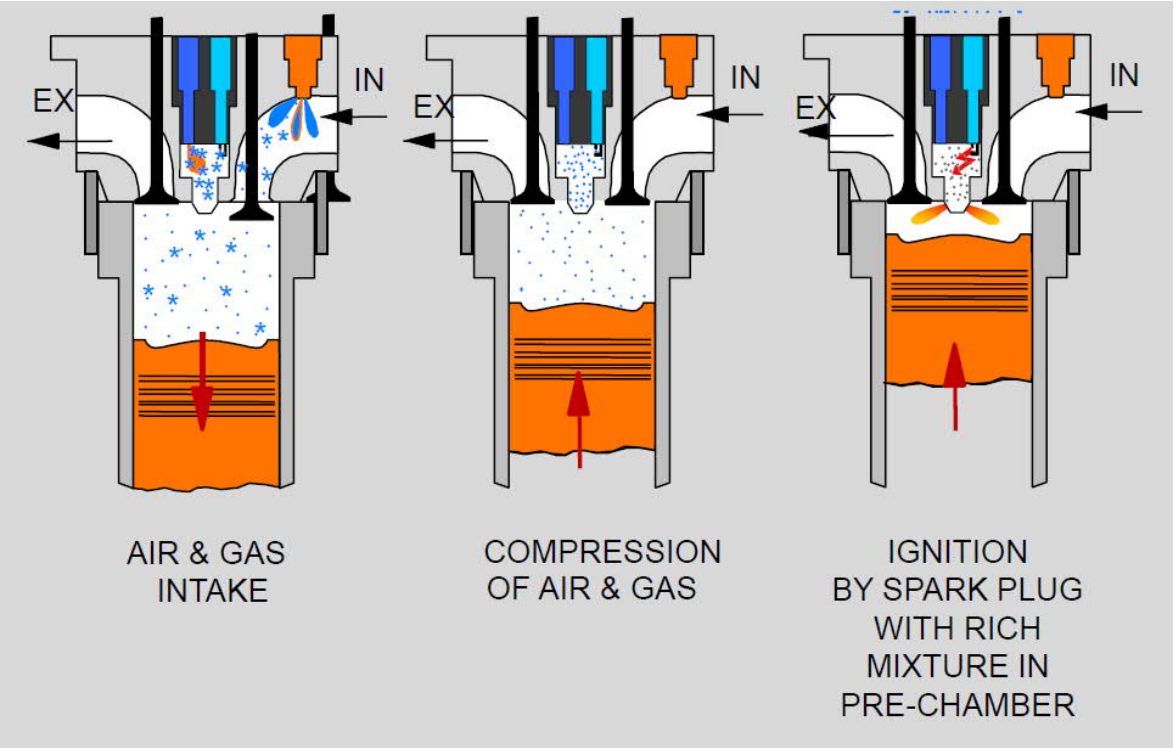

Figure 2. The operating principle of SG-series engines (Bui 2011, p. 4).

The gas admission valve located in the inlet port injects a gas mixture into the charge air. Air and fuel are then mixed and compressed in the main combustion chamber. At the same time a richer air-fuel mixture is mixed in the pre-chamber, this mixture is then ignited by a spark plug, which then ignites the leaner air-fuel mixture in the main combustion chamber. The lean-burn technology enables low exhaust emission levels and high efficiency.

2.2.2 Wärtsilä DF-series

DF stands for dual-fuel and these engines can be operated with both gaseous and liquid fuels. In diesel mode operated with liquid fuel, the engines work by the diesel cycle and compression ignition. While operating with gaseous fuel in gas mode, the combustion works in Otto cycle, triggered by a small pilot diesel injection that is approximately one percent of the total fuel amount. Operating principle of DF-series engines is illustrated in the following figure.

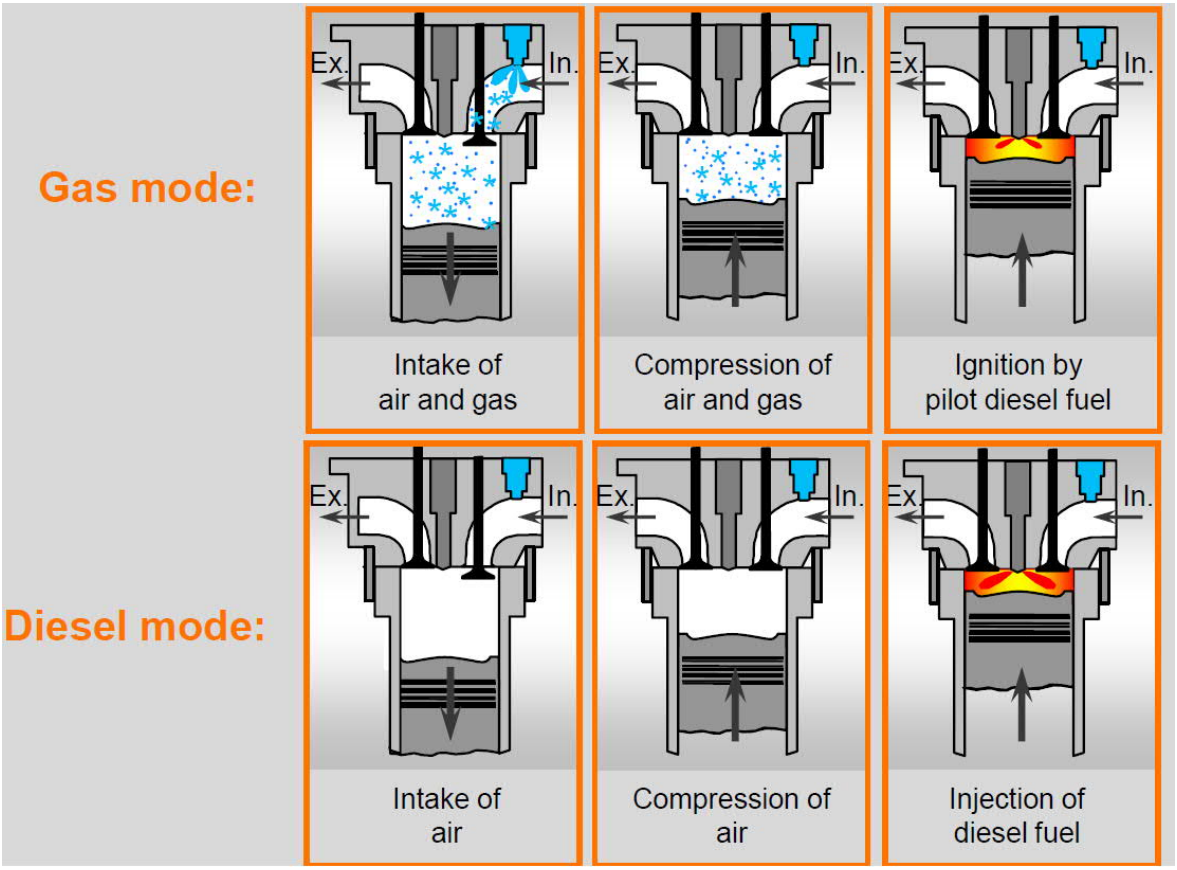

Figure 3. The operating principle of DF-series engines (Bui 2011, p. 5).

The operating principle of DF-series engines operated in gas mode is that a gas mixture is added to the charge air in the inlet port. This lean air-fuel mixture is then mixed and compressed in the combustion chamber. A small pilot injection of diesel is then injected into the combustion chamber. The temperature and pressure inside combustion chamber make the diesel fuel to auto-ignite, starting the combustion process. The DF technology offers high efficiency, fuel flexibility and low exhaust emission levels enabled by usage of gaseous fuels.

2.3 The combustion process

The combustion process of a hydrocarbon fuel is a chemical reaction that needs oxygen. For the combustion process to occur, the relative amounts of air (oxygen) and fuel must be present. Air-fuel ratio (AFR) is used to describe the mixture ratio and it is calculated on a mass basis with the following equation (Pulkrabek 2004, pp. 55-56):

$$AFR = \frac{ma}{mf} = \frac{\dot{m}a}{\dot{m}f} \quad (1)$$

Air-fuel ratio can be calculated by the total mass of air and fuel (*ma* and *mf*) or by the mass flow rate of air ($\dot{m}a$) and the mass flow rate of fuel ($\dot{m}f$). The ideal or so-called stoichiometric air-fuel ratio for natural gas is about 17:1. A lower air-fuel ratio than the stoichiometric air-fuel ratio means that the mixture is rich and a higher air-fuel ratio gives that the mixture is lean (Pulkrabek 2004, pp. 55-56).

In automotive and engine applications the ratio between air and fuel is often expressed as lambda (λ) instead of air-fuel ratio. Lambda is describing the relation between the actual air-fuel ratio and the stochiometric air-fuel ratio with the following equation:

$$\lambda = \frac{AFR_{actual}}{AFR_{s}} \tag{2}$$

The ideal mixture will give a lambda value of one, a higher value gives that the mixture is lean and a lower value gives that the mixture is rich. The air–fuel ratio of the fuel mixture will affect the efficiency of the engine and for both gasoline and gaseous fuel engines, the best efficiency is obtained with a lean mixture. The effect of air–fuel mixture for a gasoline engine is visualized in the following figure.

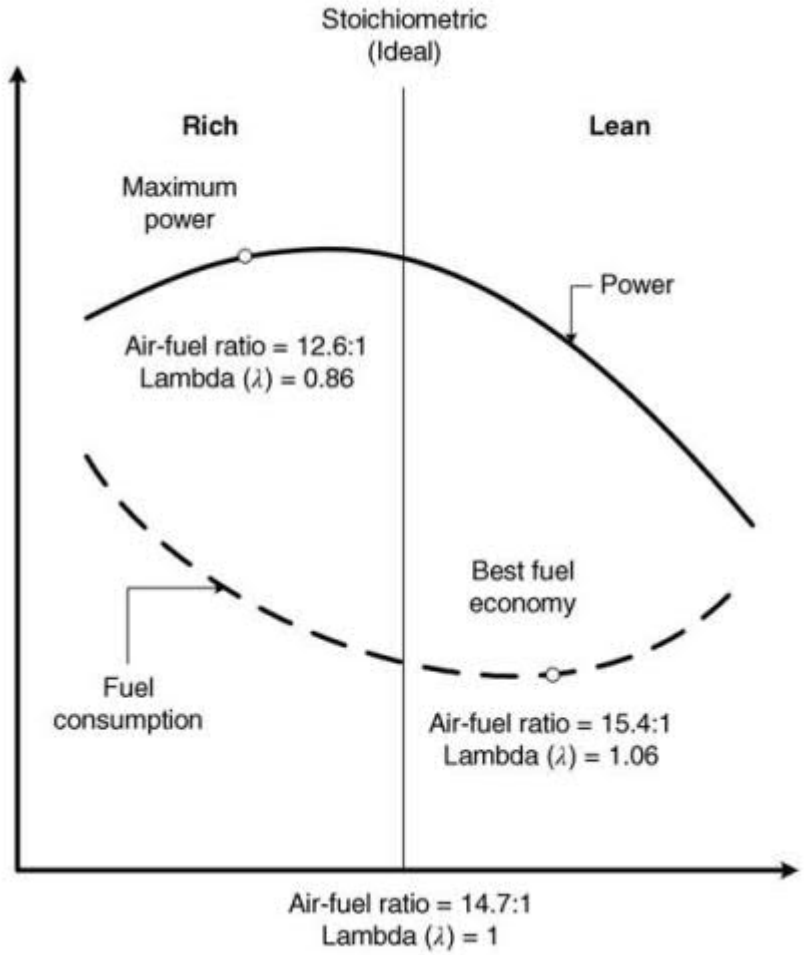

Figure 4. Effect of the air–fuel ratio in a gasoline engine (Fallah & Khajepour & Goodarzi 2016, p. 9).

Unlike gasoline engines that are normally operating on a lambda value around one, lean burn gas engines are operating at a higher lambda value, often greater than two. This is because a lean air–fuel mixture will result in a more complete combustion at lower temperatures, which will increase the efficiency of the engine and lower the exhaust emissions of nitrogen oxides, hydrocarbons and carbon monoxide.

Mean effective pressure (MEP) is a good way to compare power output between engines, because it gives the ratio of the work per cycle over the cylinder volume displaced per cycle. In other words, the mean effective pressure indicates how much work is done by the cylinder volume per cycle, which enables that engines can be compared regardless of engine size and speed. The mean effective pressure is obtained by the following equation (Fallah & Khajepour & Goodarzi 2016, p. 184):

$$MEP = \frac{P_e N_r}{V_d N_e} \quad (3)$$

Where P_e is the power produced by the engine, N_e is the number of revolutions per second, and N_r is the number of revolutions per cycle, which is two for a four-stroke engine and one for a two-stroke engine. V_d is the engine displacement that is defined with the following equation (Fallah & Khajepour & Goodarzi 2016, p. 185):

$$V_d = n\left(\frac{\pi}{4}\right) D^2 h_d \quad (4)$$

In this equation D is the cylinder bore, h_d is the stroke and n are the number of cylinders. Some commonly used mean effective pressures are indicated mean effective pressure (IMEP), brake mean effective pressure (BMEP), and friction mean effective pressure (FMEP) and the relationship between these are:

$$BMEP = IMEP - FMEP \quad (5)$$

- Indicated mean effective pressure (IMEP) indicates the work (power) produced by the combustion (Fallah & Khajepour & Goodarzi 2016, p. 186).
- Brake mean effective pressure (BMEP) indicates the useable work (power) delivered by the engine. This takes all the frictional and auxiliary losses in to account (Fallah & Khajepour & Goodarzi 2016, p. 186).
- Friction mean effective pressure (FMEP) relates to the work due to friction between moving parts of the engine (Fallah & Khajepour & Goodarzi 2016, p.186).

Another term that is used to describe the power output from an engine is engine load. It can be expressed both as actual power output in e.g. kW or in amount percent of the maximum engine power output.

2.4 Engine knock

Engine knock is an expression for a spontaneous combustion, that occurs ahead of the main flame front. This combustion is much faster than the normal combustion and it is causing local pressure pikes and pressure waves inside the combustion chamber. A metallic noise can also be heard from the engine structure. These pressure pikes caused by engine knock

can be seen on the pressure curve measured from inside the combustion chamber as visualized in the following figure (Heywood 1988, pp. 451-470).

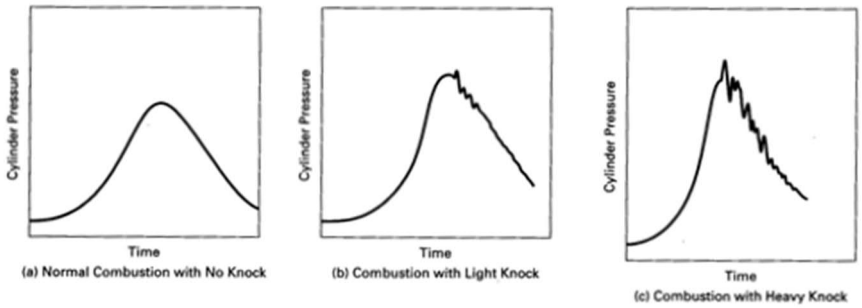

Figure 5. Differences in the combustion pressure curve between normal combustion and engine knock (Pulkrabek 2004, p. 141).

The normal combustion event in a spark-ignited engine can be described as a turbulent flame front, originating at the spark plug, moving through the air-fuel mixture in a controlled fashion dictated by the chemical kinetics of the oxidation reaction. The unburned portion of the air-fuel mixture ahead of the flame front is called “end gas”. During normal engine operation the flame propagates through the end gas, consuming the air-fuel mixture in a controlled fashion. Engine knock is an abnormal combustion phenomenon, were the end gas auto ignites and combusts before the arrival of the flame front. This produces a rapid pressure rise and extremely high localized temperatures inside the combustion chamber (Malenshek & Olsen 2008, p. 650). While mild or also called light engine knock increases fuel consumption and exhaust emissions, heavy engine knock can cause major damage on engine components and should therefore be avoided (Gupta 2013, pp. 171-183).

An engine's tendency to knock is dependent on many variables, including combustion chamber design, compression ratio, fuel properties and intake air temperature and pressure (Malenshek & Olsen 2008, p. 650). Autoignition of the end gas is connected to the pressure and temperature inside the combustion chamber and the risk of autoignition increases with rising temperatures inside the combustion chamber.

The knock resistance of the fuel is an important fuel property, since it is one of the variables that determine the knock tendency. One of the most used method for classifying the knock resistance for gaseous fuels is the methane number (MN) value. Gaseous fuels with a low methane number is more sensitive to engine knock. Definition of the methane number value and methods of determining it will be described in more detail later.

2.5 Engine misfire and the operating window

Misfiring is a term given for an incomplete or even non-existing combustion event, this is often caused by that the air-fuel mixture is too lean for ignition and this is resulting in that the combustion fails. This incomplete or even non-existing combustion event causes that the efficiency of the engine becomes lower and resulting in high hydrocarbon and carbon monoxide exhaust emissions, since unburnt fuel is exiting from the combustion chamber with the exhaust gases.

The engine is controlled to be operated optimally and in the most efficient way by the engine control system. The allowed control area is given by the operating window and the limits are placed to avoid knocking and misfiring. The operating window for a gas-fired internal combustion engine is illustrated in the following figure.

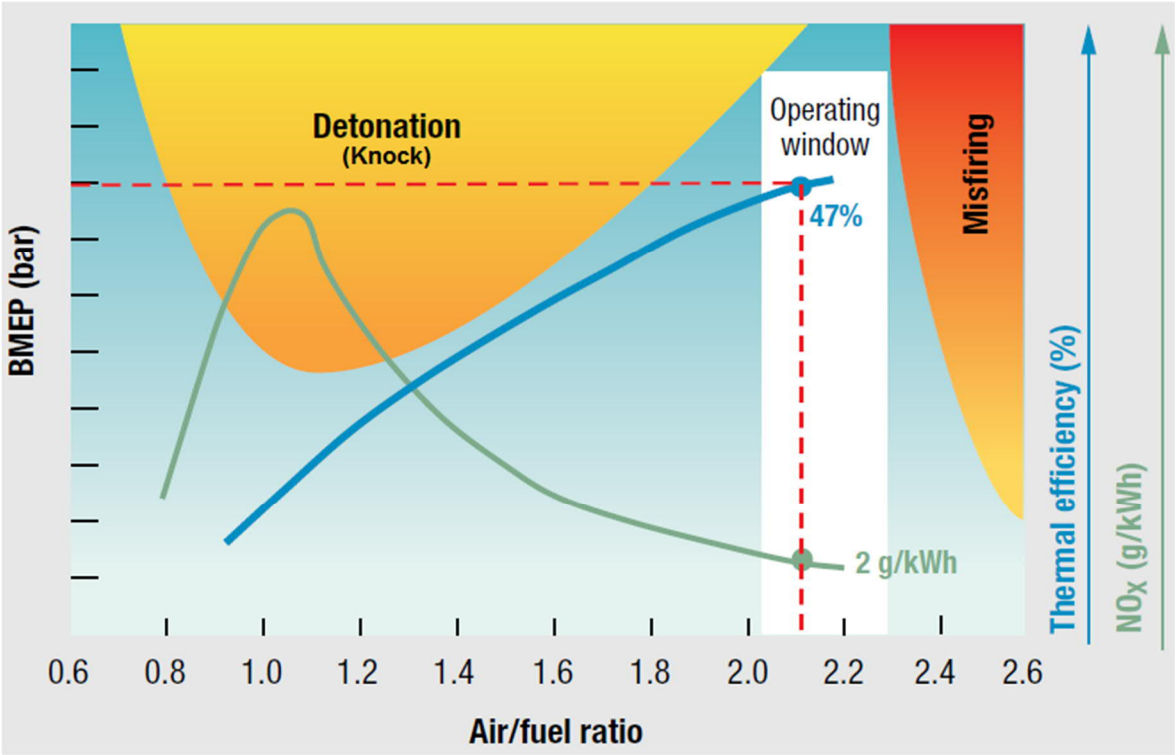

Figure 6. Operating limits for the Wärtsilä 50DF engine. (Wärtsilä 2009, p. 6).

The operating window is dependent on air-fuel ratio, but other factors such as ambient conditions, charger air temperature, compression ratio and ignition timing will also affect the operating window.

2.6 Gaseous fuel

Usage of gaseous fuels in internal combustion engines for transportation and power generation is becoming an attractive alternative to traditional fuels such as diesel and heavy fuel oil. Using gaseous fuels instead of liquid fuels can bring both environmental benefits and fuel cost savings. At the moment products from natural gas, such as liquefied natural gas (LNG) and liquid petroleum gas (LPG) are the most used types of gaseous fuels used in these applications, but there is a growing interest of using alternative gaseous fuels. This will result in larger diversity between different fuels and this will affect the combustion properties since the chemical composition of these gas mixtures are different. The following figure contains the chemical composition of some alternative gaseous fuels, that are gaining more interest to be used as fuel for internal combustion engines.

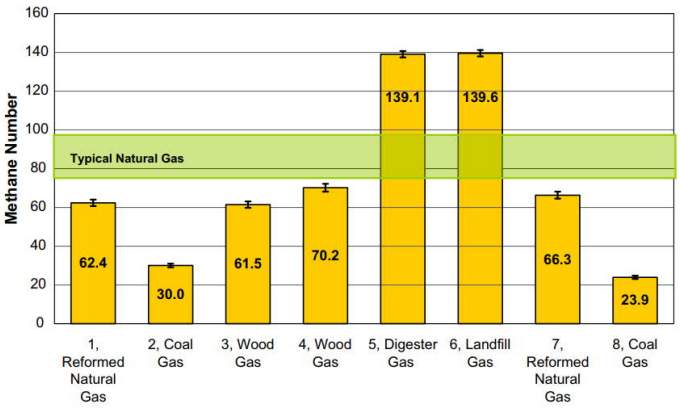

#	Test gas	Run	%CH_4	%H_2	%N_2	%CO	%CO_2	Methane number
1	Reformed natural gas		39.7	46.7	0.8	0.9	11.9	
		1	35.9	46.8	2.5	2.4	12.4	59.3
		2	38.1	44.5	2.1	2.3	13.0	62.4
		3	37.8	45.0	2.1	2.3	12.9	59.7
2	Coal gas		*	24.8	16.3	58	1	
		1	*	21.1	13.5	64.0	1.4	30.2
		2	*	22.3	13.3	63.1	1.3	30.0
		3	*	22.6	13.3	62.7	1.4	29.2
3	Wood gas		10	40	3	24	23	
		1	8.3	39.8	2.7	24.2	25.1	61.3
		2	8.3	39.7	2.4	24.3	25.3	61.5
		3	8.5	39.2	2.4	23.5	26.4	61.4
4	Wood gas		1	31	35	18	15	
		1	1.5	31.4	33.3	17.6	16.3	69.6
		2	1.6	30.9	33.8	17.4	16.2	70.2
		3	1.5	30.9	33.9	17.6	16.0	69.9
5	Digester gas		60	*	2	*	38	
		1	59.7	*	2.3	*	38.0	139.7
		2	60.8	*	1.5	*	37.8	139.1
		3	60.5	*	1.5	*	38.0	138.5
6	Landfill gas		60	*	*	*	40	
		1	60.3	*	*	*	39.7	139.7
		2	60.5	*	*	*	39.5	139.6
		3	60.5	*	*	*	39.5	139.5
7	Reformed natural gas		1.2	30.8	49.0	15.6	3.4	
		1	1.8	30.8	50.4	13.7	3.3	57.3
		2	1.4	30.2	47.4	13.9	7.1	66.3
		3	1.6	30.1	47.1	14.0	7.3	65.6
8	Coal gas		7	44	*	43	6	
		1	6.3	44.5	*	43.2	6.0	24.8
		2	6.6	44.4	*	42.9	6.1	23.9
		3	6.3	44.7	*	42.9	6.1	23.3

Figure 7. Components of different gaseous fuels. (Malenshek & Olsen 2008, p. 654).

Modern internal combustion engines are often designed for gas mixtures with a methane number of 80 or above to achieve a high-power density, low exhaust emission levels and high efficiency. Lower quality gaseous fuels can result in poor combustion, misfire and engine knock. The engine control system must adapt to these variations in the fuel quality to maintain high efficiency, minimum exhaust emission levels, but most important a safe and reliable operation of these engines. Natural gas is widely used as fuel in internal combustion engines for transportation and power generation and the following figure contains the chemical composition of natural gas.

Component	Typical analysis (vol%)	Range (vol%)
Methane	94.9	87.0–96.0
Ethane	2.5	1.8–5.1
Propane	0.2	0.1–1.5
Isobutane	0.03	0.01–0.3
n-Butane	0.03	0.01–0.3
Isopentane	0.01	Trace to 0.14
n-Pentane	0.01	Trace to 0.14
Hexane	0.01	Trace to 0.06
Nitrogen	1.6	1.3–5.6
Carbon dioxide	0.7	0.1–1.0
Oxygen	0.02	0.01–0.1
Hydrogen	Trace	Trace to 0.02

Figure 8. Chemical composition of natural gas (Demirbas 2010, p. 60).

2.7 Gaseous fuel quality

Variations in gaseous fuel composition present several challenges for engine operation. The variations in the composition influences the ignitability and the combustion behaviour of the gas mixture (CIMAC 2015, p. 4). The property of different gas mixtures can be described by the following quantities that are presented below.

An important property of the fuel is the energy content and it is expressed as higher heating value (HHV) and lower heating value (LHV), these are also called gross and net calorific value. The difference between these two is the latent heat of condensation of the water vapour in the combustion exhaust gas. The higher heating value takes into account the latent heat of vaporization of water in the combustion products and considers that water stays liquid. On the other hand, the lower heating value does not take this into account and consider that water leaves in gas state and the energy required to vaporize the water therefore is not released as heat. In brief the lower heating value is obtained by subtracting the heat of vaporization of the water from the higher heating value. The lower heating value is almost exclusively used in engine applications, since the combustion products of an internal combustion engine are all in the gaseous state (Heywood 1988, pp. 78-79).

Wobbe index (WI), also called Wobbe number of a gaseous fuel is determined by its composition and it is a measure of the interchangeability of gaseous fuels and their relative ability to deliver energy. Wobbe index, I_W is the ratio of higher heating value of the gaseous fuel divided by the square root of the specific gravity and it is calculated with the following equation (Ramadhas 2012, p. 231):

$$I_W = \frac{V_C}{\sqrt{G_S}} \tag{6}$$

In this equation V_C is the higher heating value, and G_S is the specific gravity of the gas mixture. The ISO 6976:2016 standard specifies methods for calculating gross calorific value, net calorific value, density, relative density, gross Wobbe index and net Wobbe index of natural gases. This standard specifies that Wobbe index in common usage and in absence of any other qualifier refers to gross Wobbe index. Net Wobbe index, which is calculated with the net calorific value (LHV) is calculated with the following equation (ISO 6976:2016):

$$I_{W(net)} = \frac{V_{C(net)}}{\sqrt{G_S}} \tag{7}$$

The Wobbe index is directly proportional to the heating value of gas that flows sub-sonically through the orifice in response to a given pressure drop. Changes in the Wobbe index will result in nearly proportional changes in the rate of energy flow and air–fuel ratio. This results in that the energy output will be identical for two gaseous fuels with the same Wobbe Indices, when the pressure and valve settings are identical (Ramadhas 2012, p. 231).

Possibly the most important fuel property for gaseous fuels used in gas-fired engines is the methane number. The methane number value provides an indication of the knock tendency of the gaseous fuel, like octane number for gasoline. To ensure reliable and economic operation of gas-fired engines, the knocking characteristic of the used gaseous fuel must be known. This often results in that the composition of the gas mixture must be measured in order to determine the methane number, since suppliers of natural gas often only specifies the heating value and Wobbe Index of the gas. Unfortunately, there is no good correlation between heating value or Wobbe Index and the methane number for natural gas. (CIMAC 2015, p. 7). Gas composition measurement techniques and calculation methods of the methane number value are described later in chapter 4.

3 Relating researches

Wärtsilä have already for several years worked on different development projects relating to the gas quality measurement technology and engine control dependent on gas quality. In addition to internal development work, there has been two master's theses written in connection to these subjects.

3.1 Online gas quality measurement and engine control

Jacob Grönroos at Aalto University wrote in 2016 a master's thesis named "Online gas quality measurement and engine control". The focus of his research was placed on the sensing technologies of the gas quality. This included testing of the MKS Precisive gas analyzer and its communication to other control systems. There was also research done on identification of different possible control methods based on gas quality and the methane number value of the gas.

The outcome of his research was that the MKS Precisive gas analyzer is suited for continuous gas quality monitoring purposes and could be used for engine control functions based on the methane number (Grönroos 2016).

3.2 Measures to utilize real-time gas quality analyses for engine control

A second master's thesis in connection to the gas quality technology was written in 2018 by Dennis Högberg at Åbo Akademi University. This master's thesis is named "Measures to utilize real-time gas quality analyses for engine control" and focus was put on to further testing of the MKS Precisive gas analyzer by analyzing measurement data from operating power plants that is already using this measurement equipment. Another measurement equipment besides the MKS Precisive gas analyzer was also evaluated. This MEMS Qs Flonic sensor does not measure the composition in the gas mixture directly. Instead it determines thermal conductivity, heat capacity and density of the gas mixture. Properties of the analyzed gas mixture, such as calorific value and methane number can then be calculated, since there is a correlation between these. (Högberg, 2018)

In this research it was found out that the accuracy of the MEMS Qs Flonic sensor is not good enough for gas quality monitoring purposes and engine control, so the MKS Precisive gas analyzer remains as the preferred option for these purposes. It was also concluded and recommended that future development work should be put on to implement a control

function based on the gas methane number. Research should also be done on the influence of measurement location and lag time in the complete measurement chain (Högberg, 2018).

This present master's thesis acts as a sequel to these two-mentioned master's theses and continues the research work connected to these subjects. The main objective is to design and implement the control function in form of a controller. The influences of measurement location and response time of used measurement equipment are also in the scope for this thesis work, since they need to be considered for the design of the controller dynamics.

4 Gas quality measurement principles

This chapter will describe the determination procedure of the gas methane number. The methane number value of a gaseous fuel gives an indication of the gas quality and it is calculated from the gas mixture composition. The supplier can often provide the gas mixture composition, but measurement of the composition can also be needed if is unknown. Therefore, this chapter starts with the measurement principle of the MKS Precisive gas analyzer and then reviewing different methane number calculation methods.

4.1 Tunable filter spectrometer gas analyzer

The MKS Precisive gas analyzer uses a tunable filter spectrometer measurement method and the sensor consist of a light source, a sample cell, a wavelength separating element (spectrometer) and a photo-detector (MKS Instruments, n.d. a). The construction of a tunable filter spectrometer sensor is illustrated in the following figure.

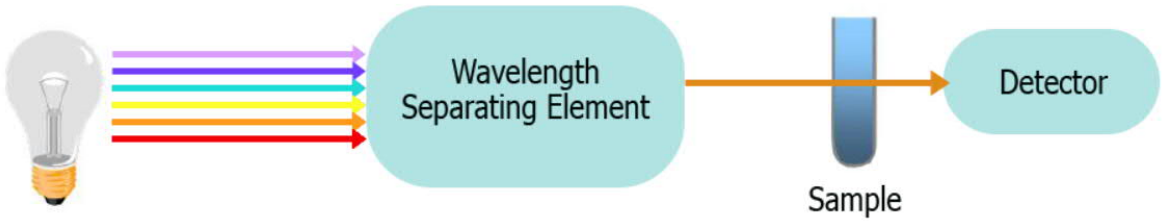

Figure 9. The construction of a tunable filter spectrometer sensor (MKS Instruments, n.d. a).

A tunable filter spectrometer measurement device uses a wavelength separating element that first "slices" the wavelength components of the broadband light source before it interacts

with the molecules from the gas that is being analyzed. Some of the wavelength components are absorbed and others are transmitted through without any absorption. The resulting spectrum is called absorption spectrum and it acts as "fingerprints" which are used to identify components of the gas sample and quantifies the composition of the sample (MKS Instruments, n.d. a). The principle of the tunable filter spectrometer method is illustrated in the following figure.

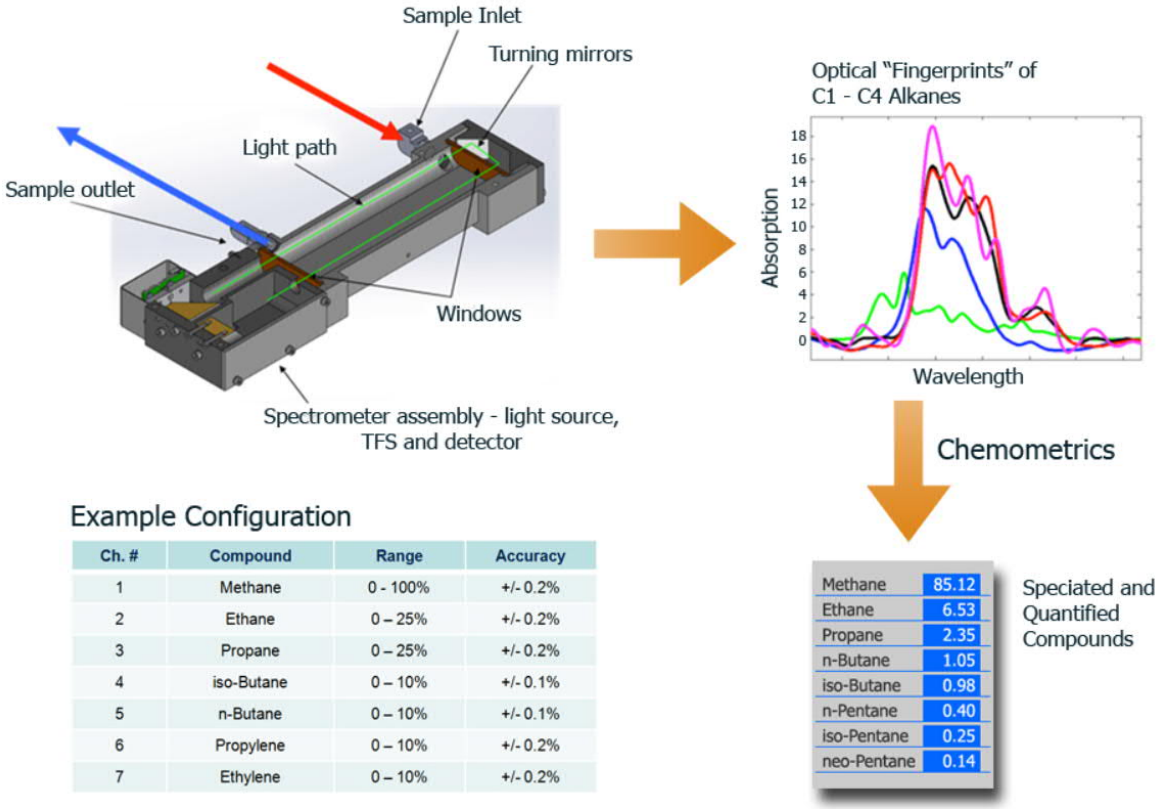

Figure 10. Measurement method of the tunable filter spectrometer (MKS Instruments, n.d. a).

This acquired spectrum is both in the ultraviolet and infrared regions, which enables identification possibilities of many different components and makes it suitable for many different applications. Some of possible applications are displayed in the following figure.

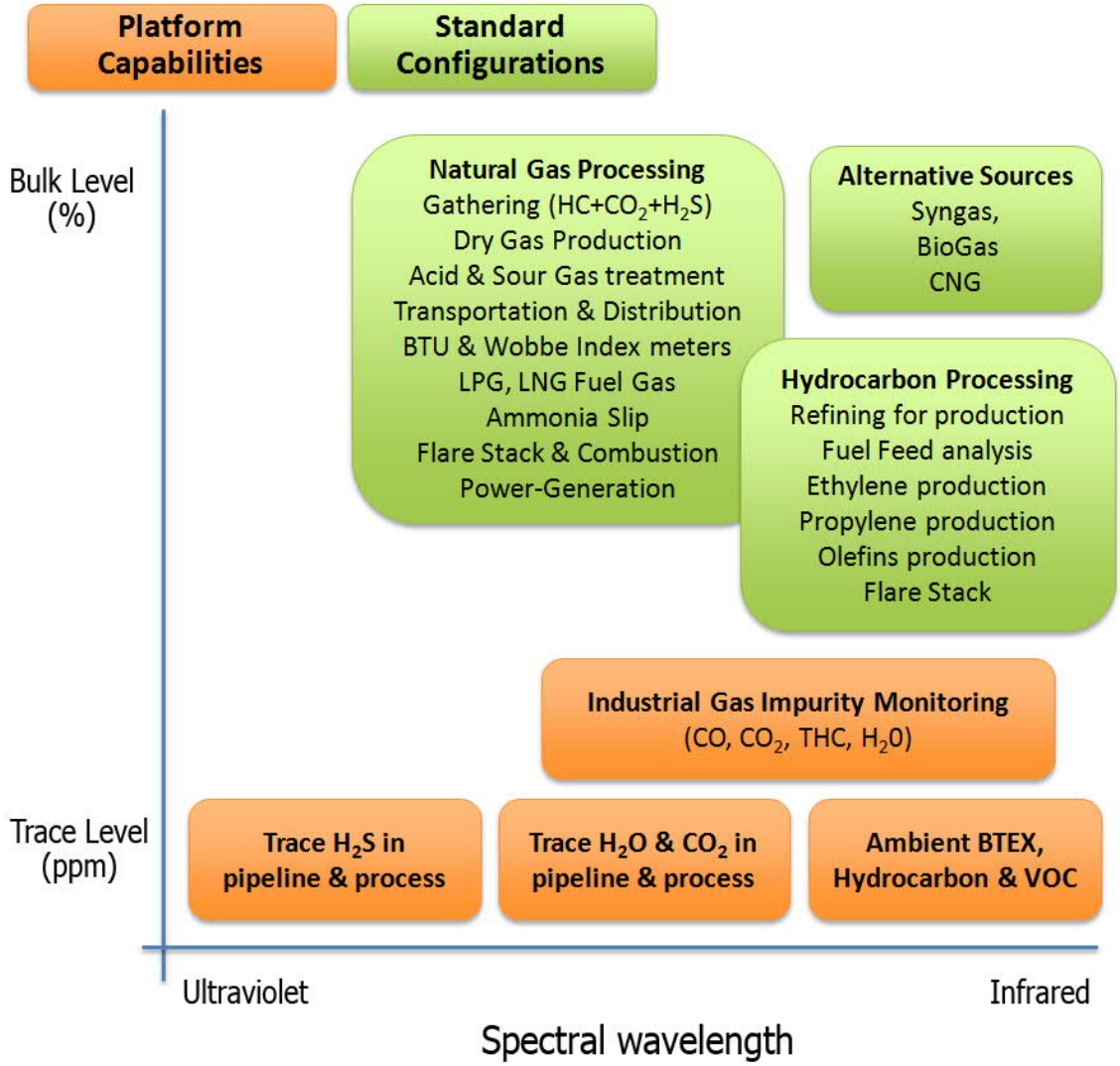

Figure 11. Wavelength spectral regions and possible applications (MKS Instruments, n.d. b).

In addition to the identification possibility of different components in the gas mixture, it can also calculate the superior calorific value and Wobbe index of the analyzed gas mixture, these both quantities are of interest in combustion control applications.

A common limitation for spectrometers is identification of diatomic elements, such as nitrogen (N_2) and hydrogen (H_2). This has been solved by that the gas analyzer gives a balance reading by calculating together all other gas components and subtracting them from the total volume (100 %) (Grönroos 2016, pp. 20-21). The balance reading can then be used for estimating amount of nitrogen in the gas mixture, but this requires that there is no hydrogen present. This measurement equipment enables continuous measurement of the gaseous fuel with good accuracy, but at the same time with low maintenance and low operational cost compared to more expensive devices like gas chromatography instruments

and is therefore a suitable measurement equipment for gaseous fuel analysis in engine control applications.

4.2 Methane Number

There is until now no standard available for gaseous fuel knock rating, but the methane number of a gaseous fuel provides an indication of the knock tendency and is therefore often the preferred unit used for classifying the knock resistance of gaseous hydrocarbon-based fuels.

The definition of methane number is that pure methane (CH_4) has a methane number of l00 and pure hydrogen (H_2) has a methane number of O (Andersen 1999, p. 3). This originates from that methane, which has a high knock resistance and is therefore given an index value of 100 and hydrogen, which burns quickly relative to methane, has a low knock resistance and is given the index value of 0. However, there are some inert gases that increases the methane number and it is therefore possible for a gas mixture to have higher methane number than 100, e.g. landfill biogas that mainly contains of methane and carbon dioxide has often a methane number greater than 100.

There are several different calculation methods of methane number available, but the base for methane number calculation comes from studies performed by the Austrian company AVL in the late sixties. These studies include gas components like CH_4, C_2H_4, C_2H_6, C_3H_6, C_3H_8, $n-C_4H_{10}$, H_2, CO_2, N_2 and H_2S in binary and ternary component mixtures (Andersen, 1999). The results from the AVL studies are available as ternary diagrams, as illustrated in the following figure.

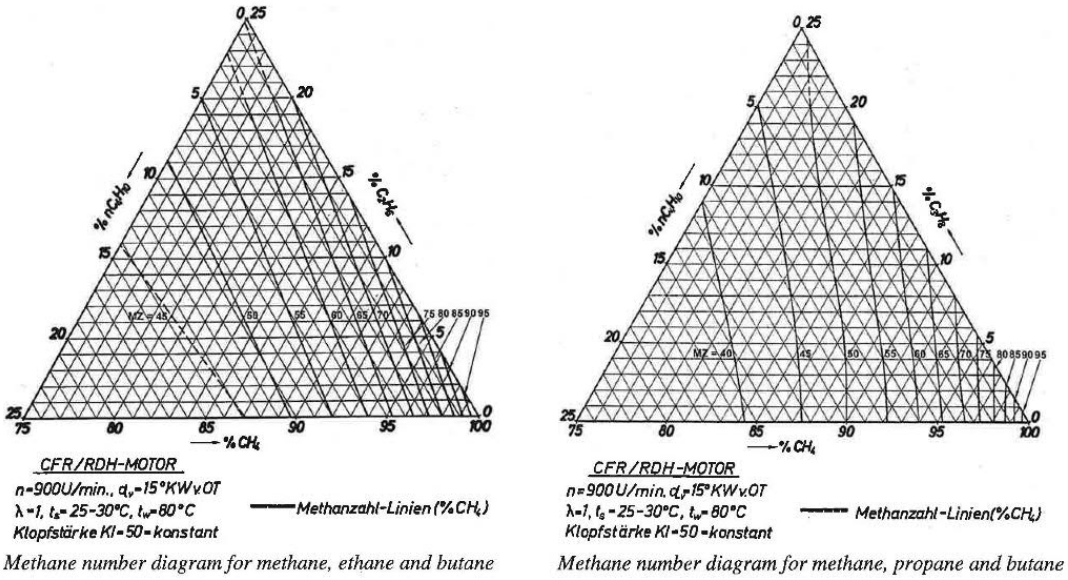

Methane number diagram for methane, ethane and butane *Methane number diagram for methane, propane and butane*

Figure 12. Methane number diagram for different gas components (Leiker M, Christoph K, Rankl M, Cantellieri W, Pfeifer U, 1972).

Most of methane number calculation methods available today is based on an algorithm that is performing a complex interpolation procedure using the ternary diagrams from the AVL studies. The lack of information in the AVL studies regarding the impact of higher hydrocarbons has led up to that some methods has implemented modifications to the basic calculations based on their own tests with higher hydrocarbons in order to cover a wider range of real-world fuel composition (CIMAC 2015, pp. 5-6).

4.3 Wärtsilä methane number

The Wärtsilä methane number (WMN) was developed in cooperation with DNV GL and the motive for the development was to get a better method suitable for modern engine design that characterizes the knock resistance for a broader range of fuels. (DNV GL, 2015)

The Wärtsilä methane number uses a method to characterize gases for their knock resistance based on the fuel mixture combustion properties. This is done by an algorithm that is based on two models. The first model is an engine thermodynamic model and this model is predicting how the pressure and temperature in unburned end gases changes during the engine cycle. Verification of this model has been done with extensive engine testing with different gas mixtures. The second model is an autoignition model of different gases and this model is used to predict the autoignition behaviour of different gaseous fuels. The model is based on autoignition delay time tests in a rapid compression machine (RCM) (van Essen &

Gersen 2015, pp. 4-6). The following figure illustrates the pressure trace from an autoignition delay time test performed in a rapid compression machine.

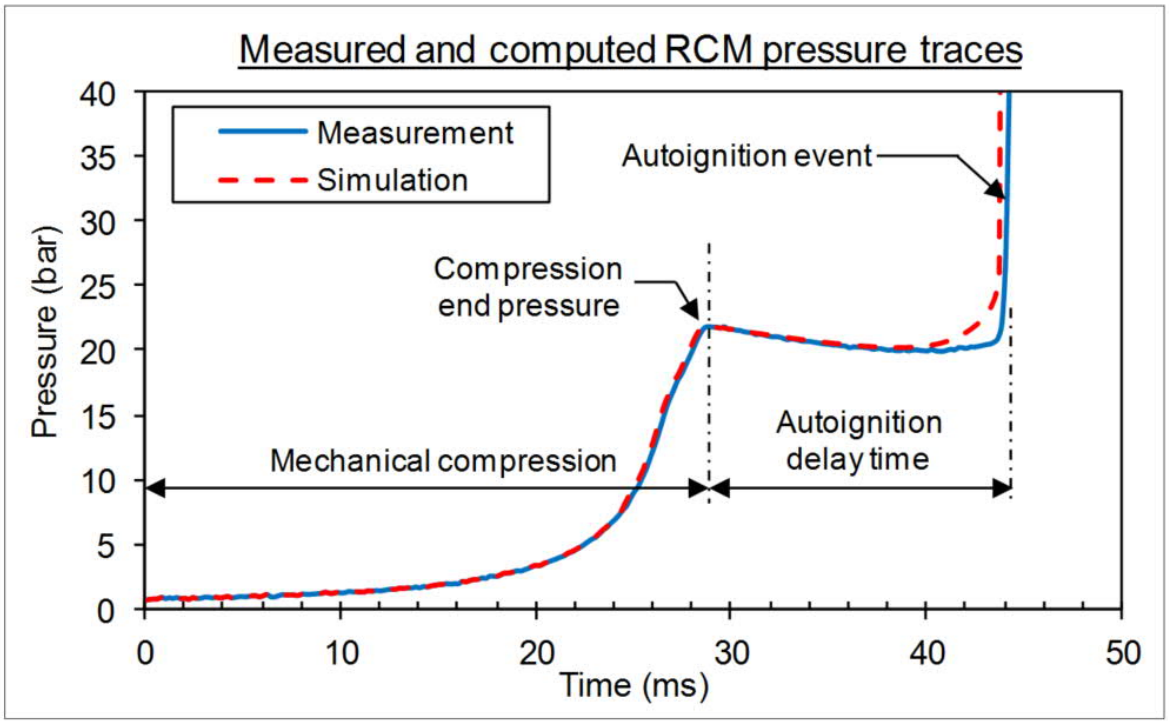

Figure 13. RCM pressure trace (van Essen & Gersen 2018, p. 11).

A n-pentane-based scale is then used to compare the knock resistance of different gases with each other. This scale is defined, so that the knock resistance for a given gaseous fuel mixture is expressed as an equivalent fraction of n-pentane in methane and it is referred to as Wärtsilä knock index (WKI).

A second scale is also used to compare the knock resistance, and this is a propane-based scale. This scale is referred to as propane knock index (PKI) and the knock resistance for a given gaseous fuel mixture is expressed as an equivalent fraction of propane in methane under identical engine conditions. Results from a comparison test with the standard methane number method, which is known as the AVL method and the propane knock index is presented in the following figure. (van Essen & Gersen, 2015).

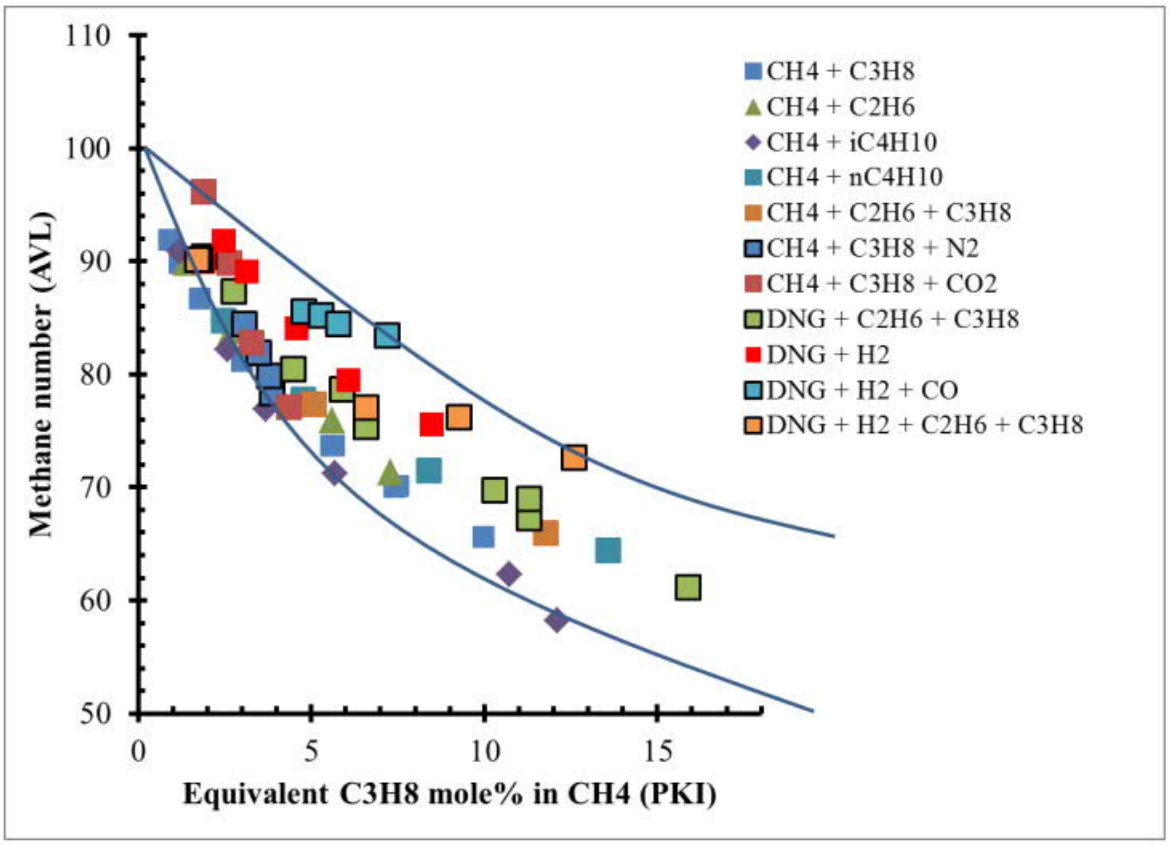

Figure 14. Methane number (AVL 3.2) versus PKI for different gas mixtures (van Essen & Gersen 2015, p. 8).

With measurement data from engine testing it has been concluded that the n-pentane based scale (WKI), is a more suitable scale to rank the knock resistance, especially on lower engine loads that are lower than 70 percent. This is illustrated in the following figure and it can be seen that with the n-pentane based scale (WKI), the autoignition delay time still decreases with increasing n-pentane fraction at lower loads compared to effect on lower loads with the propane-based scale (PKI). With this scale the resulting reduction of the autoignition delay time only changes slightly when adding more propane to the fuel mixture.

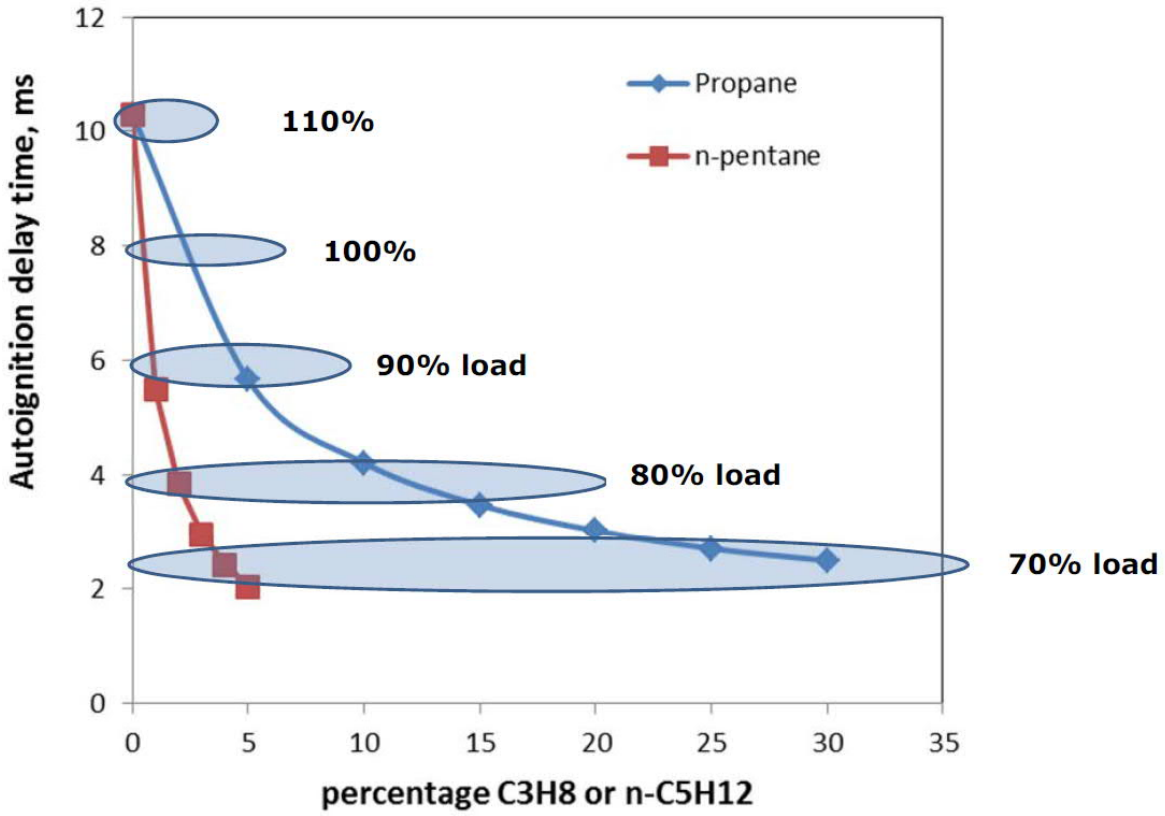

Figure 15. Calculated autoignition delay times at a constant temperature (940K) and pressure (120 bar) for WKI and PKI (van Essen & Gersen 2018, p. 21).

To get the n-pentane based scale (WKI) similar to other gaseous fuel knock resistance rating methods it is converted to a normalized knock index on a 0-100 scale, and this gives the Wärtsilä methane number (WMN). This method of calculating methane number has been proven better suitable for modern engine design and supports a broader range of fuels, therefore this is the method used in this thesis and all quantities of methane number is calculated by this method.

5 Model-based design with Simulink PLC coder

In 2010 MathWorks launched a new product named Simulink PLC Coder. The Simulink PLC Coder generates hardware-independent IEC 61131 structured text code from Simulink models, state flow charts, and embedded Matlab functions for industrial control systems. This enables model-based design for process equipment controlled by PLCs and PACs. Many PLC manufactures supports programming with structured text, but there can be some small differences between different manufactures. At the time of writing the Simulink PLC coder fully supports products from e.g. Rockwell Automation, Siemens and Omron and MathWorks is currently working on to release support for products from Schneider electric. The Simulink PLC coder function requires that the model is containing only blocks that are supported by the Simulink PLC coder.

5.1 IEC 61131 Standard

The International Electrotechnical Commission (IEC) recognizes five standard programming languages for PLCs in their IEC 61131 standard. They are Ladder Diagram (LD), Function Block Diagram (FBD), Sequential Function Chart (SFC), Instruction List (IL) and Structured Text (ST). The Simulink PLC coder generates ST code and therefore there is a short introduction to this programming language.

5.2 Structured text programming language

The structured text programming language is text-based unlike most other PLC programming languages that are graphics-based, such as ladder diagram or function block diagram. In the following figure the difference between four PLC programming languages is shown.

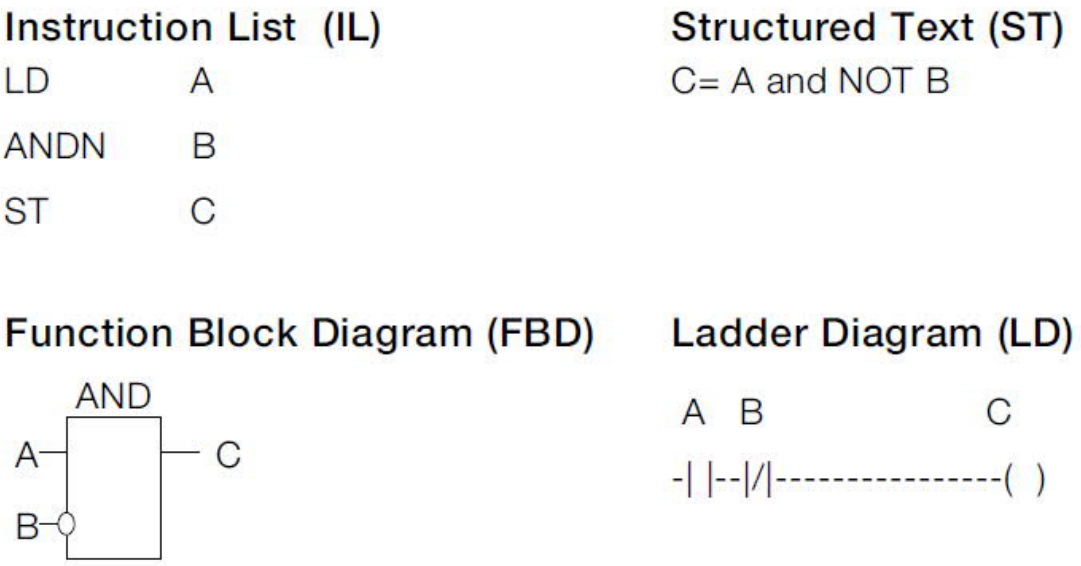

Figure 16. Same function in four different PLC programming languages.

A benefit of using the ST programming language is that the ST code can relatively easy be copied between different PLC types and manufactories. Another benefit of using non-graphical programming languages, such as ST or IL is that they run much faster than graphics-based programming languages. There are some disadvantages of using the ST programming language, one of them is that troubleshooting can be more complicated, since many feel that text environment is somewhat unfamiliar and troubleshooting of the code can be more complicated than graphics-based programming languages (Bosch Rexroth Corporation, 2009).

Many PLC manufacturers allow that ST code can be encapsulated into a block, so that it can be used in graphics-based programming languages. This enables that the model-based design approach can be used also for graphics-based programming languages. However, it is important that the ST code is thoroughly tested and verified, so it is bug-free, since the code is somewhat hidden and not so easy accessible.

5.3 Model-based design

Model-based design can be very helpful when designing a controller or a control function for a process. Requirements can be validated and the feasibility of a project can be determined by conducting early tests and verification checks. Rapid prototyping can be performed by testing the design against a model of the environment and the plant. After this simulation test has been successfully conducted, ST code can be generated from the

controller model to test it against the actual plant and environment. The actual workflow for the model-based design approach is illustrated in the following figure (Aarenstrup, 2015, pp. 5-10).

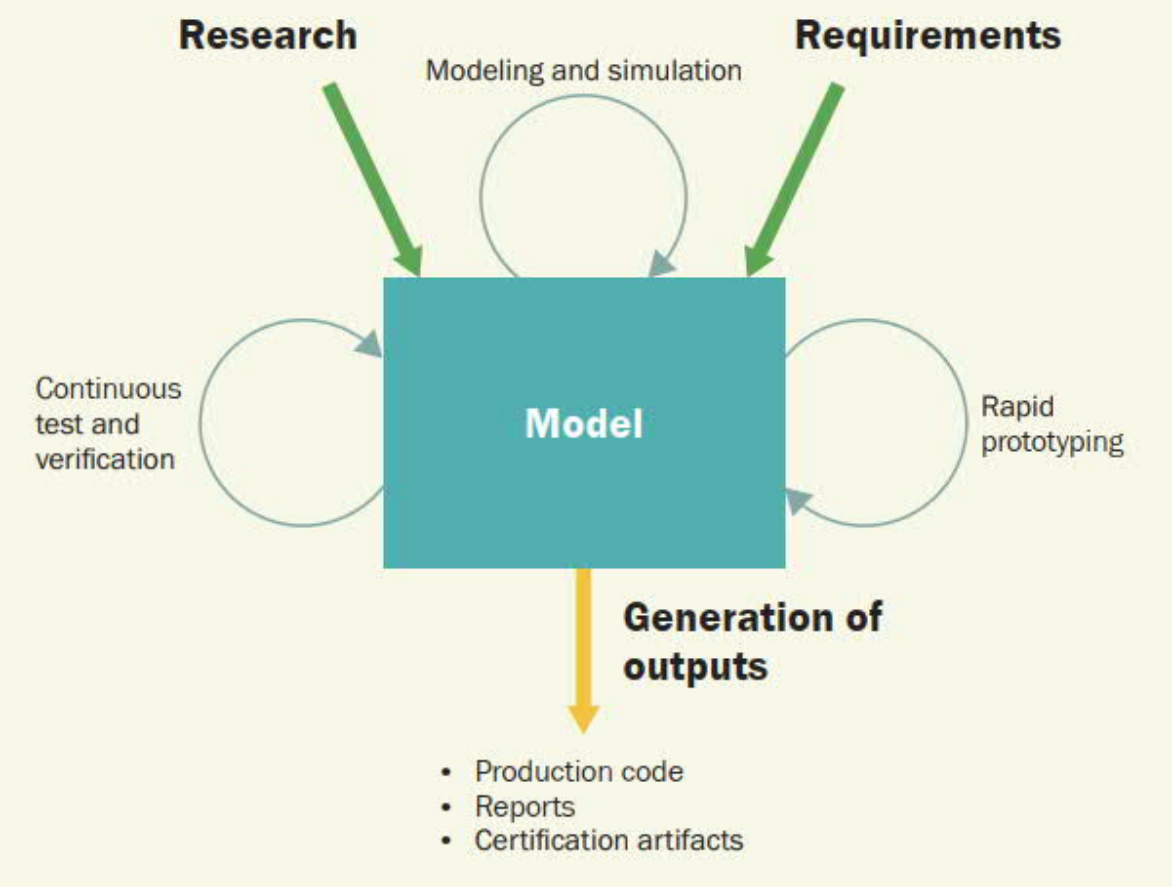

Figure 17. Workflow for the model-based design approach (Aarenstrup 2015, p. 5).

Some of the benefits with model-based design are that it helps to manage complex systems and it enables that new ideas can quickly be explored. Design problems and uncertainties can be investigated early, since continuous test and verification is done at every stage of development process, which results in that faults are identified as soon as they are introduced into the design. This helps to eliminate errors and reduces overall development and validation time (Aarenstrup 2015, pp. 5-10).

The Simulink PLC Coder also provides code optimization routines, which reduces the memory size and increases the execution speed of the generated structured text and ladder diagrams. The behaviour and execution of the ST code is verified against the model simulation behaviour. Simulink also offers generation of C and C++ code for real-time systems and software-based PLC solutions.

6 Control of max allowed power output

The definition of derating in engine applications is to reduce the power output of the engine from its nominal output. There are different reasons for derating an engine, most common reason of derating is to match the ambient air conditions on the installation site. Sometimes engines are derated to ensure optimum efficiency by restricting the power output, resulting in lower fuel consumption. Engine derating can also be done to protect the engine and other process equipment from mechanical damage, e.g. by avoiding heavy knocking. The derating techniques between diesel and gas engines are different, but the focus in this thesis will mainly be on the derating methods used on gas-fired engines in Wärtsilä's SG-series.

6.1 Current derating of gas engines

Currently there are three different curves used to define the derating factor. These are dependent on charge air temperature and methane number, incoming gas pressure to the engine and the engine suction air temperature. Parameters such as methane number of gas on site, lower heating value of gas (LHV) and site altitude (barometric pressure) are often predetermined in the projects. There are three derating factors defined from these curves and these three derating factors are called K_{KNOCK}, K_{GAS} and K_{TC}. These factors are independent of each other and the max allowed power output from the engine is calculated from the lowest value of the derating factors.

6.1.1 Derating due to charge air receiver temperature and methane number

The first derating factor K_{KNOCK} comes from a combined curve dependent on the charge air receiver temperature and the gas methane number. The reason for derating is to avoid engine knock. There are different curves available depending on the emission level that is required for the engine installation. The following figure displays an example of a K_{KNOCK} derating curve for the Wärtsilä 34SG engine.

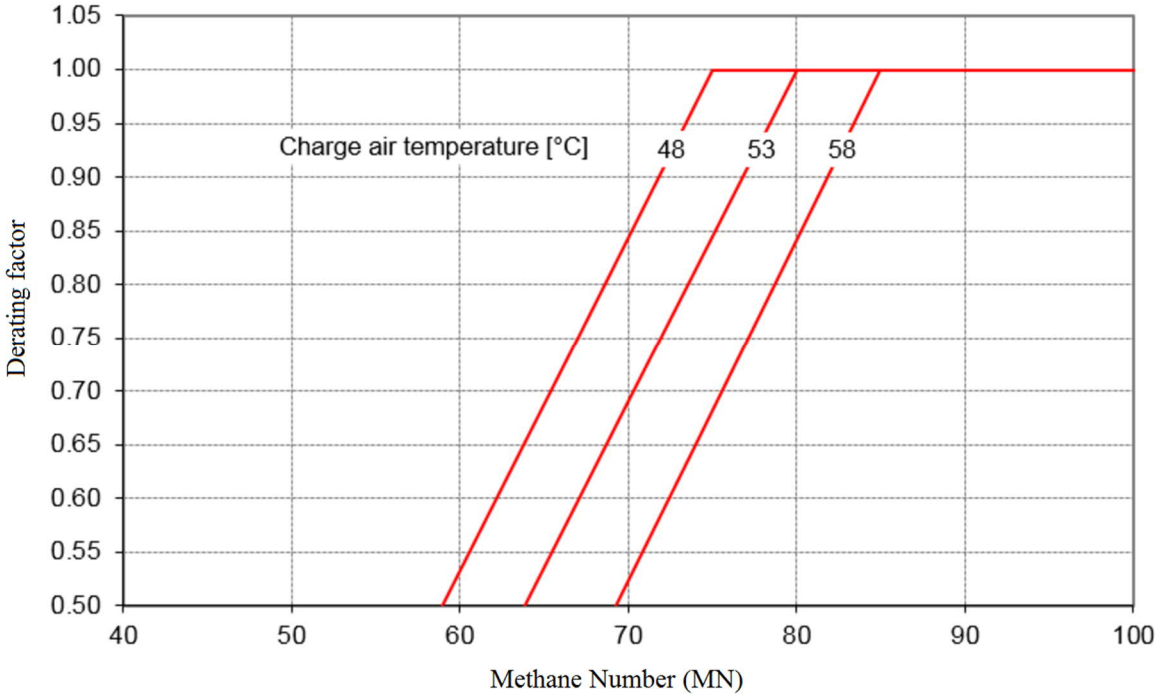

Figure 18. Wärtsilä 34SG K_{KNOCK}derating curve (Wärtsilä 2015).

In practice in current installations, the gaseous fuel methane number is predetermined in the project phase, so the curve that is used for controlling the engine has the charge air receiver temperature on x-axis instead of methane number. This modified curve is displayed in the following figure.

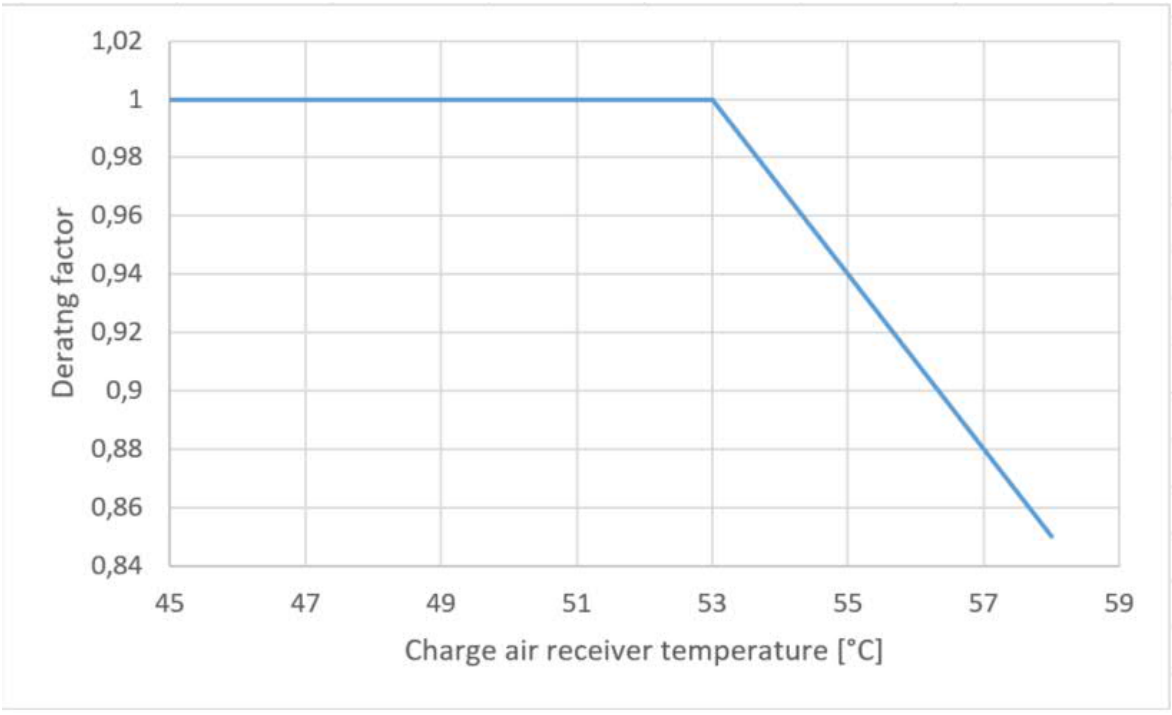

Figure 19. Wärtsilä 34SG K_{KNOCK}derating curve for MN 80.

This will change in future installations, due to the MN_derating controller that is presented in this thesis work. By using this controller, there will be a better control off the engine when there is changes in the gas methane number of incoming gas, since it considers the actual continuous measured gas methane number for calculating the derating factor in K_{KNOCK} curve.

6.1.2 Derating due to LHV of gas and gas feed pressure into engine.

The second derating factor K_{GAS}takes in to consideration the lower heating value of the gas used as fuel and the gas feed pressure. The reason for derating is that, if there is not enough feed pressure of gas supplied to the engine, which leads to that not enough fuel can be supplied to the engine and it cannot run its rated power output. The required gas feed pressure is depending on the lower heating value of the gaseous fuel. The following figure displays an example of a K_{GAS}derating curve for the Wärtsilä 34SG engine.

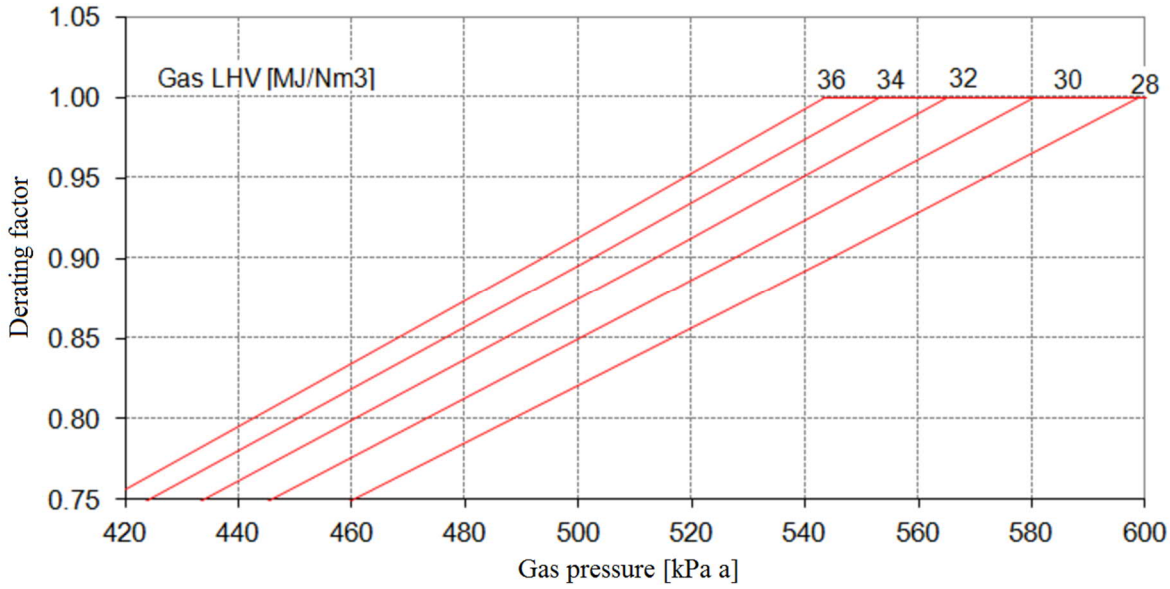

Figure 20. Wärtsilä 34SG K_{GAS}derating curve (Wärtsilä 2015).

The lower heating value of gas is also predetermined in the projects phase in current installations. The gas quality measurement technology enables that actual lower heating value of gas can be determent in real time and this makes it possible to have a dynamic derating control also for this derating factor in future installations.

6.1.3 Derating due to ambient air pressure and suction air temperature.

Turbocharged engines use a turbocharger to supply the engine with air for the combustion process and changes in ambient conditions have an immediate effect on turbocharger performance, due to decreasing air density and pressure with increasing altitude. This results in that pressure ratio across the turbine increases as the ambient air pressure goes down and that is resulting in a higher turbocharger speed. Intake temperature of the turbocharger also has an effect, since the needed energy to compress the air is directly proportional to the intake temperature. Therefore, at a given turbocharger speed, the pressure ratio of the compressor decreases with increasing intake temperature. The purpose of the K_{TC} derating factor is to protect the turbocharger and prevent it from overspeeding. The following figure displays an example of a K_{TC} derating curve for the Wärtsilä 34SG engine.

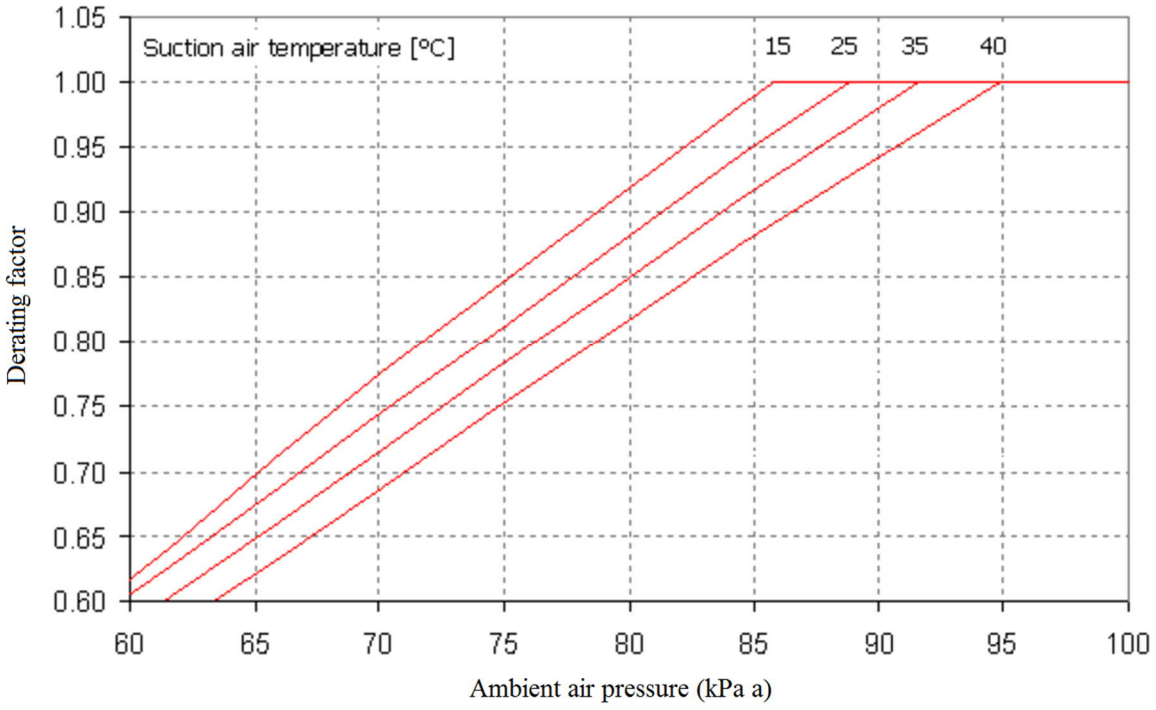

Figure 21. Wärtsilä 34SG K_{TC} derating curve (Wärtsilä 2015).

The ambient air pressure can be predetermined in the project phase, since it is connected to the ambient conditions of the installation location, such as altitude and local variation and is mostly quite constant. This resulting in that the K_{TC} derating factor can be decided by just considering the suction air temperature.

7 MN_derating controller

This chapter will cover the functionality of the MN_derating controller. This controller controls the maximum allowed power output dependent on the gas methane number and it determines if the engine should be derated to maintain safe operating condition with varying gas quality. The layout of MN_derating controller can be seen in the following figure.

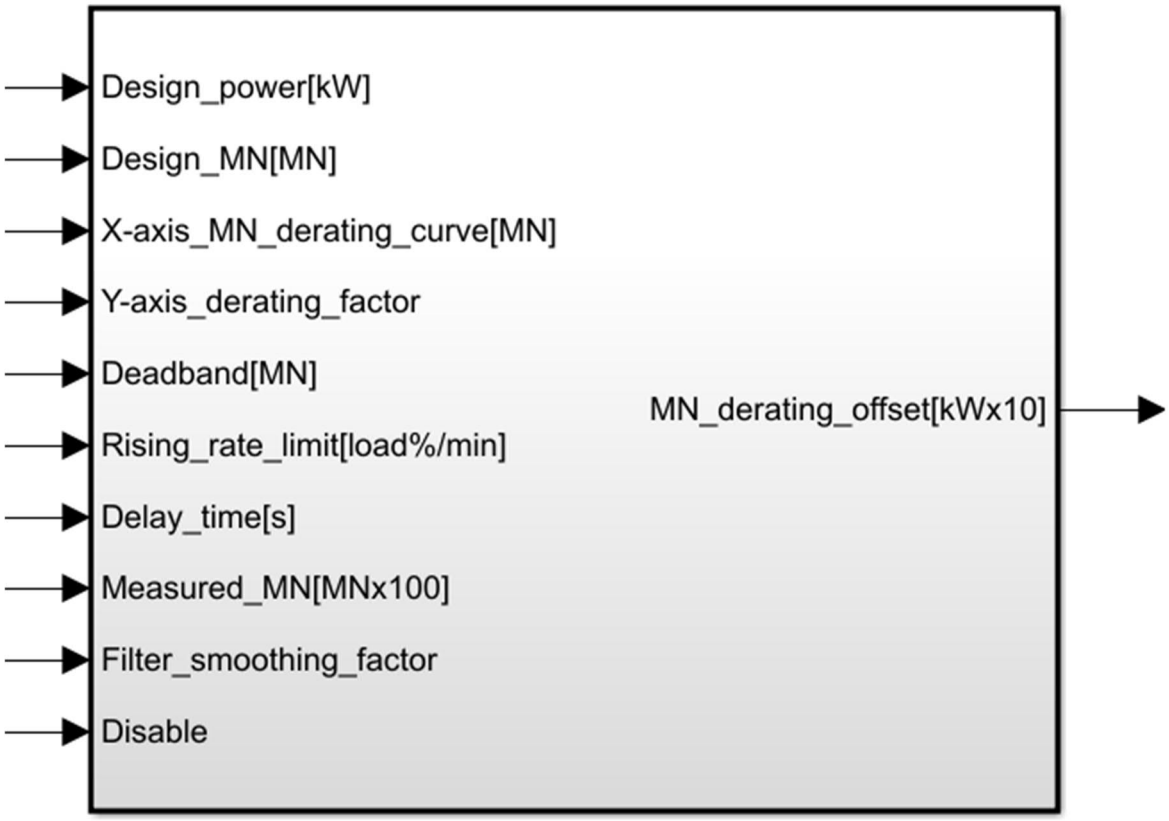

Figure 22. Layout of the MN_derating controller.

The scope of this work includes the complete design phase from identification of the functionality to final product. This chapter will cover all the steps in the design process from identification to final product, which includes functionality identification, solutions for signal filtering, impact of other engine control functions and response time of used measurement equipment.

7.1 Requirements specification

A requirements specification is used to identify the wants and needs in the project and it should e.g. describe the functionality of the product or system. All requirements are defined

in the beginning of the project, preferably before the development process has started. This specification will then act as support during the development process and contribute that the final product fulfils its targets. In this thesis work there are three different types of requirements used and these are:

- Functional requirements define a function of the system or its components. A function is described as a set of inputs, the behaviour, and outputs and they are used to define in detail what the system is supposed to accomplish (Robertson & Robertson 2012).

- Quality requirements are specifications of the quality of the product. In this case where the objective is to develop a control function in an automation system, the most important quality requirements are usability and performance (Robertson & Robertson 2012).

- Design constraints define limitations in the design. In this case they consist of quality control testing and timing constraints, where development schedule is the most important one (Robertson & Robertson 2012).

The requirements specification for the controller that is developed in this thesis work is presented in appendix 1.

7.2 Influence of other control functions

In this chapter it will be investigated how the active load limitation control based on the gas methane number will influence other engine control functions. It is critical to evaluate how different control functions affect each other to get an overall good working control system.

7.2.1 Dew-point control

Water can start to condensate from the engine charge air and this is most common in locations with high air humidity ratio. This can become a problem and most of the condensation happens in the charge air cooler where air that is going into the engine is cooled down. There is a dew-point control available that can be used to prevent this from happening.

The dew-point control rises the temperature of the engine charge air in order to prevent excessive condensation in the charge air cooler, which can result in corrosion of engine components and in worst case even water strokes.

This means that a high humidity ratio leads to a higher receiver temperature, which increases the knocking tendency of the engine, but at the same time, the high humidity ratio decreases the knocking tendency. These two effects partly cancel out each other and therefore in these situations a higher charge air temperature can be allowed without increasing the engine knocking tendency.

The K_{KNOCK} derating curve is normally adjusted in these situations where an engine is operated in a location with a high air humidity ratio. The derating breakpoint is adjusted to allow a higher receiver temperature without that the engine starts to derate. An example of an adjusted K_{KNOCK} derating curve can be seen in the following figure.

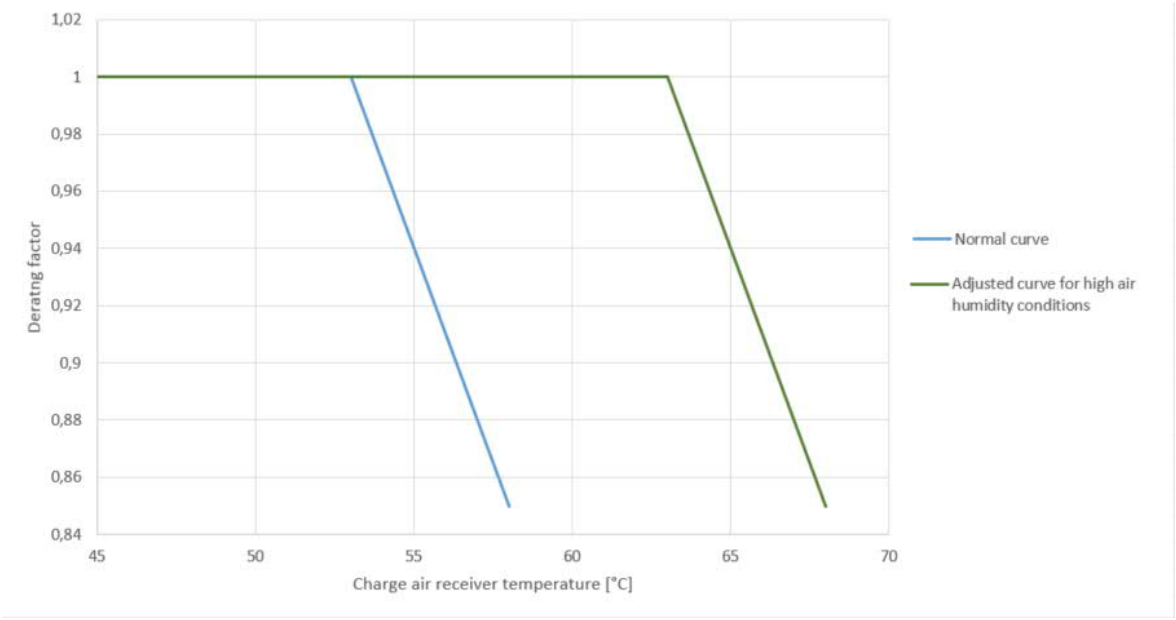

Figure 23. Comparison between the normal and an adjusted K_{KNOCK} derating curve.

7.2.2 Fuel sharing control

Fuel sharing is a function that is available for dual fuel engines. Normally a dual fuel engine that is operating in gas mode means that gaseous fuel is used as primary fuel and only a small part of liquid fuel is used as ignition source. The fuel sharing control enables that the engine

can be operated with both gas and liquid fuel as primary fuels, e.g. 50 percent of the total fuel amount is gaseous fuel and 50 percent is liquid fuel. Fuel sharing is available on Wärtsilä DF-series engines and the benefit of this function is that a higher power output from the engine can be allowed even with a gaseous fuel of worse quality with lower methane number, which would normally restrict the power output from the engine. The following figure illustrates the allowed window for the fuel sharing control.

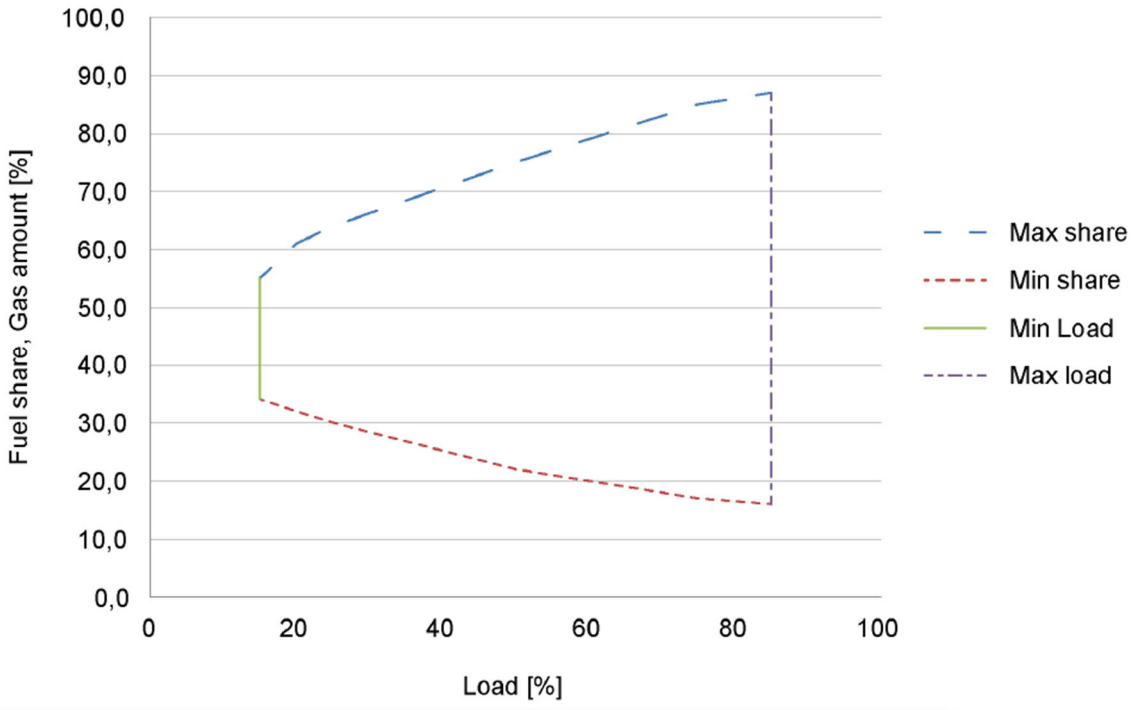

Figure 24. Allowed fuel sharing window for Wärtsilä 50 DF engines (Wärtsilä 2018, p. 14-9).

The idea with fuel sharing is that the liquid fuel is used to cover portion of needed energy for maintaining a high-power output and that the engine does not need to be derated. For this to function properly, it means that the MN_derating controller should be disabled, when fuel sharing control is enabled. There is a disable input available in the MN_derating controller and when this input is true the MN_derating controller is disabled and the output goes to zero.

7.3 Signal filter design

There is no signal filtration done on the measured gas component signals coming from the gas analyzer. The methane number calculation is done directly on the raw signals coming from the gas analyzer. This results in that it might be necessary to perform some filtration

on the calculated methane number signal, since this signal is used for controlling the engine. The following figure shows an example off the unfiltered calculated methane number signal.

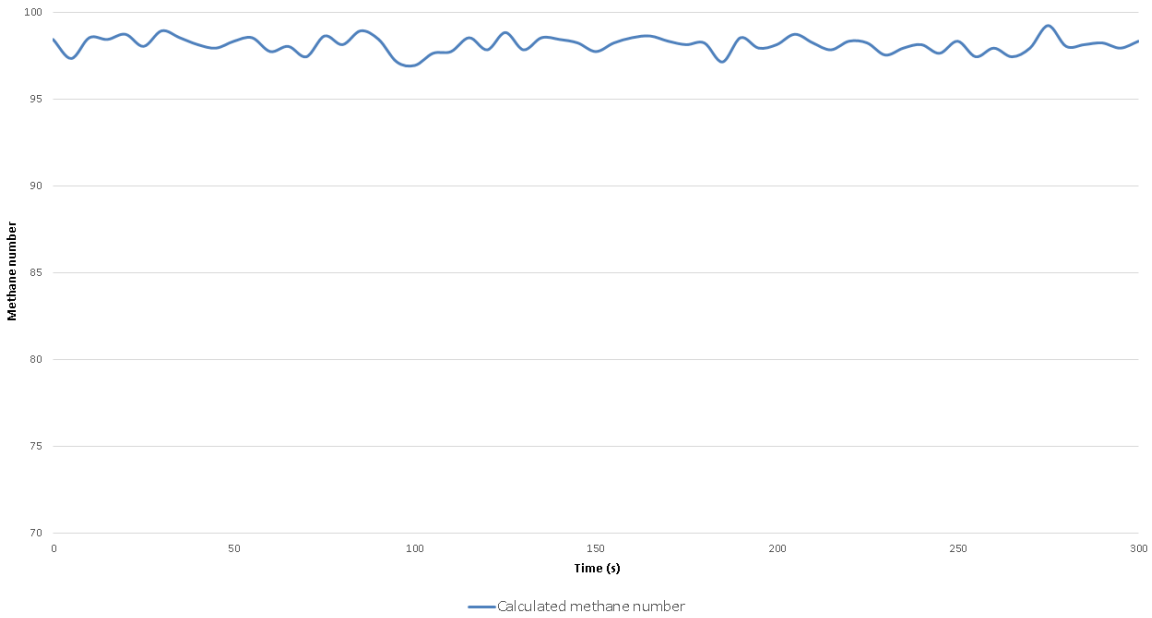

Figure 25. Unfiltered methane number signal.

The unfiltered methane number signal in Figure 25 is overall steady with only some minor fluctuations. This indicates that the signal only needs to be smoothed a little bit with some light filtration. A frequency spectrum analysis of this signal is done to better understand what kind of filter is needed. In the following figure the single-sided power spectrum is displayed for the unfiltered methane number signal showed in Figure 25.

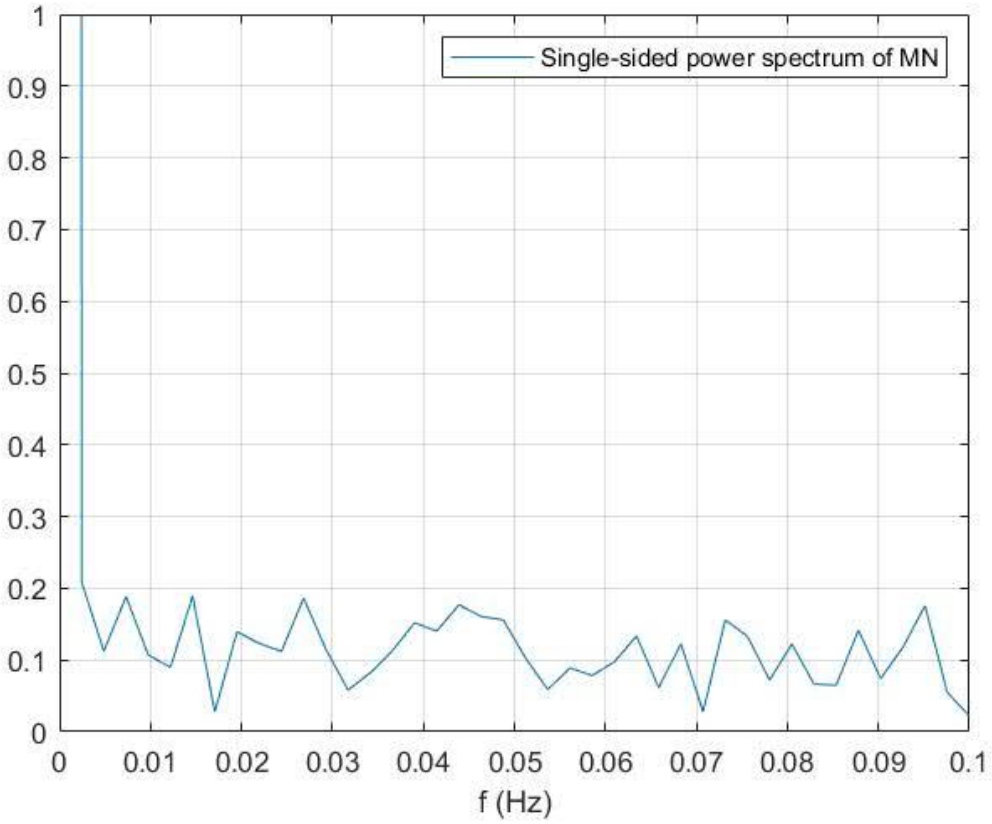

Figure 26. Single-sided power spectrum of the methane number signal.

The use of a digital low pass filter is not suitable for this application, since taking in to consideration the low sampling rate from the gas analyzer, where the sample frequency is only 0,2Hz and this can also be seen from the frequency spectrum analysis in Figure 26. Instead some kind of moving average filter is to be preferred and therefore three different average filters will be evaluated in the following chapters.

7.3.1 Moving average filter

A moving average filter operates by averaging a number of data points from the input signal to generate an output signal. The moving average filter is a simple filter that is good for reducing noise in the input signal and still retaining a sharp step response. The equation for the moving average filter is presented below (Smith 1999, pp. 277-284):

$$y[n] = \frac{1}{M} \sum_{k=0}^{M-1} x[n-k] \tag{6}$$

In this equation, x [] is the input signal, y[] is the output signal and M is the number of sample points used to calculate the moving average. In this application a one-sided average

calculation can only be used, because the input signal to the filter is a continuous calculated signal from measured data from the process. This leads to that only the current and older data points can be used for calculating the average value (Smith 1999, pp. 277-284). In the following figure the effect of a moving average filter can be seen, with different amount of data points used for calculating the average value.

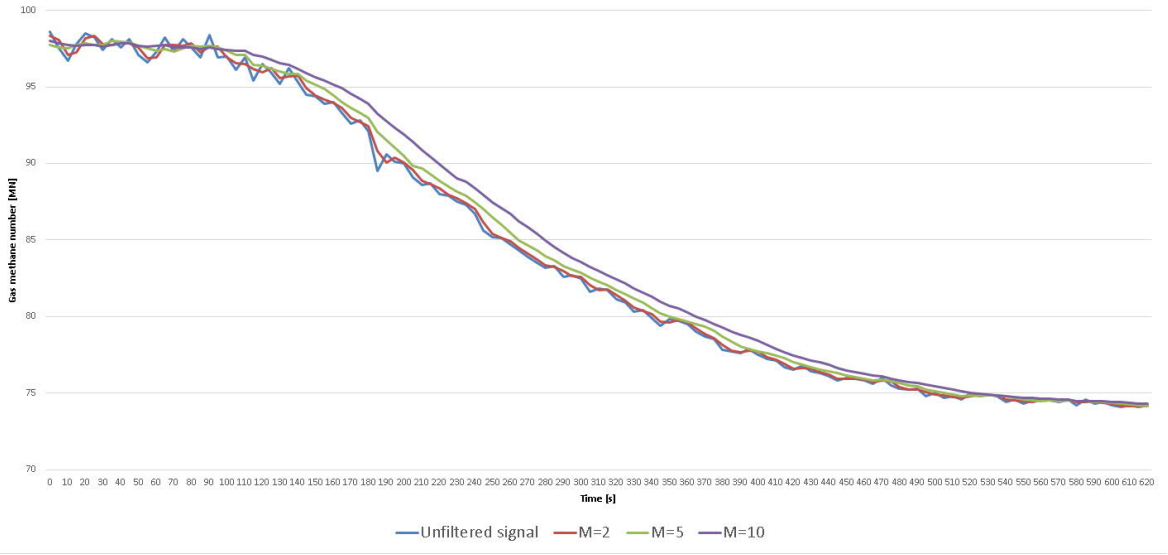

Figure 27. Signal filtration with a moving average filter.

When a larger number of sample points are used the smoothing effect is better, but it will give a larger relative shift between the input and output signals. This relative shift between the input and output signals is one of the biggest disadvantages for this kind of filter.

7.3.2 Weighted moving average filter

The difference between a standard moving average filter and a weighted moving average filter is that the weighted moving average filter has multiplying factors to give different weights to data at different positions in the sample window. This filter weights recent data more heavily than older data, which results in a less aggressive filter, with a better phase response, that gives a smaller shift between the input and output signals. The weights decrease in arithmetical progression and in the following figure the different weights are displayed for a five sample point weighted averaging filter (Smith 1999, pp. 277-284).

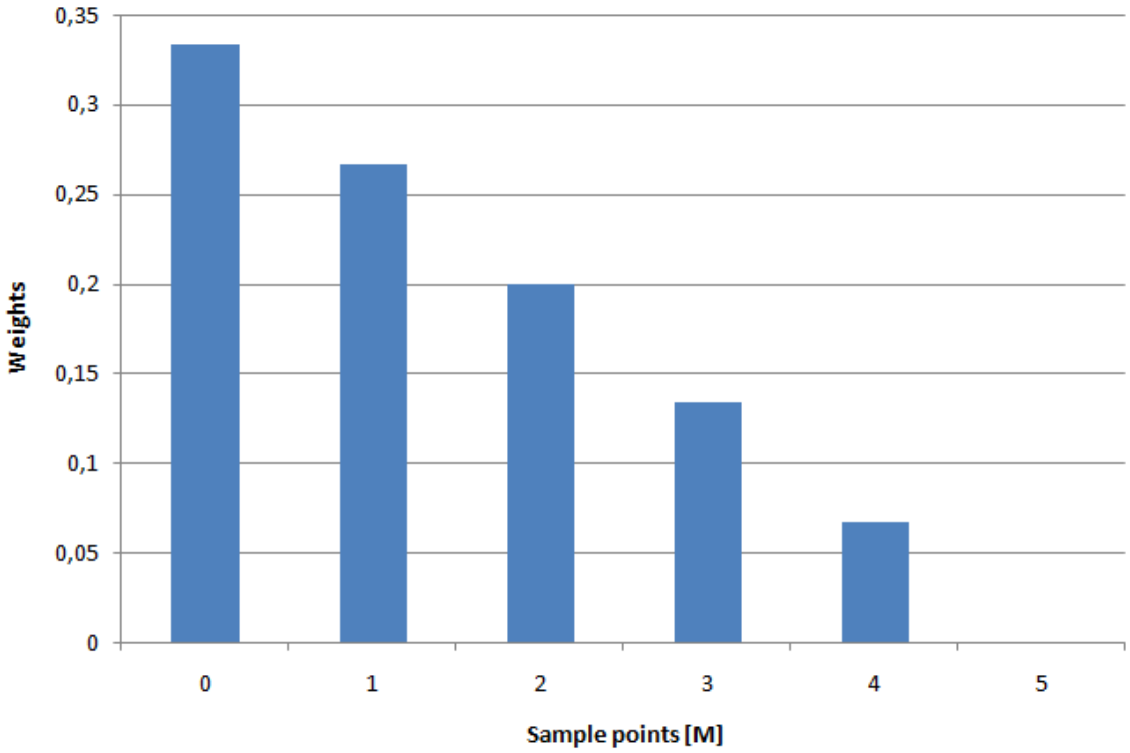

Figure 28. Weights for a five data point weighted moving average filter.

The weighted moving average filter is described by the following equation:

$$y[n] = \frac{1}{S}\sum_{k=0}^{M-1}\omega_k x[n-k] \tag{7}$$

Where ω_k is the decreasing function of *k* and denotes the weight given to the input *x[]* and *S* is the normalization constant chosen so that the sum of all filter coefficients equals to one. These parameters are described by the following equations (Smith 1999, pp. 277-284):

$$\omega_k = (M - k) \tag{8}$$

$$S = \frac{M(M+1)}{2} \tag{9}$$

In the following figure the effect of the weighted moving average filter can be seen, when the same amount of data points, as for the standard moving average filter is used.

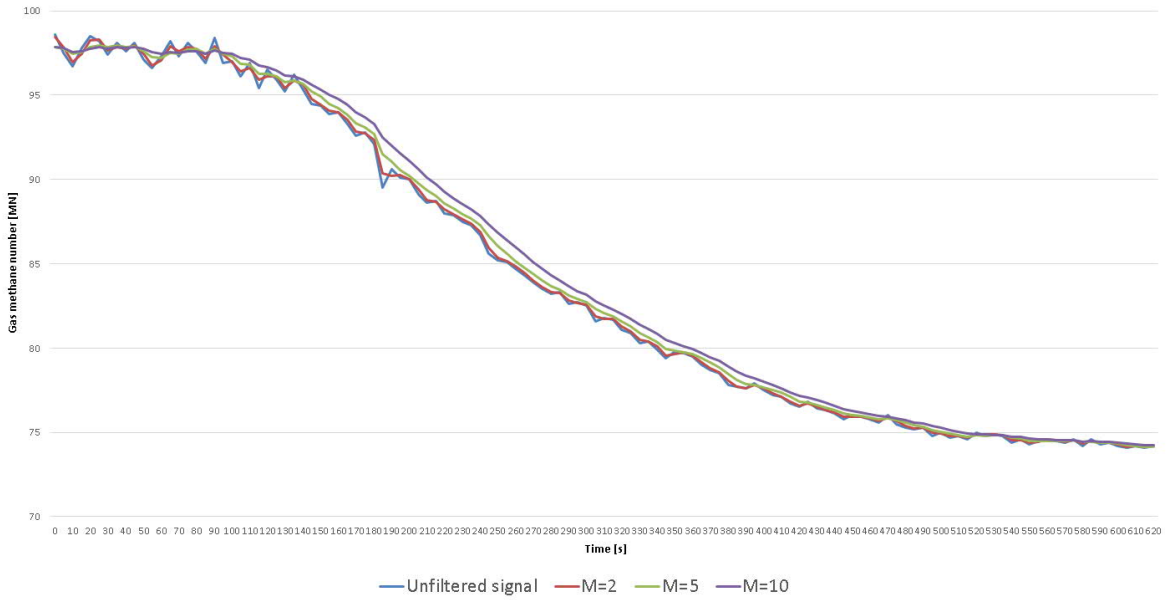

Figure 29. Signal filtration with a weighted moving average filter.

Compared to the standard moving averaging filter it can be seen from the figure that the phase response is better for the weighted moving averaging filter.

7.3.3 Exponential smoothing filter

This filtering method is mostly known as the Brown's simple exponential smoothing method, but it can also be referred to as the single exponential smoothing method and it is basically a method to perform an exponentially weighted moving average. In the same way as for the standard weighted moving average filter this filter also gives larger weights to more recent data, but the weights decrease exponentially as the observations become more distant. The Brown's simple exponential smoothing method is described by the following equation (Brown 1963, pp. 99-104):

$$S_t[x] = \alpha x_t + (1-\alpha) S_{t-1}[x] \tag{10}$$

This will give an exponentially weighted average of the current observation x_t and the previous smoothed statistic S_{t-1}. The smoothing factor α is a value between 0 and 1, a larger value of α reduces the level of smoothing, where if α = 1 the output signal is just the current input signal. The effect of smoothing factor α can be seen in the following figure (Brown 1963, pp. 99-104).

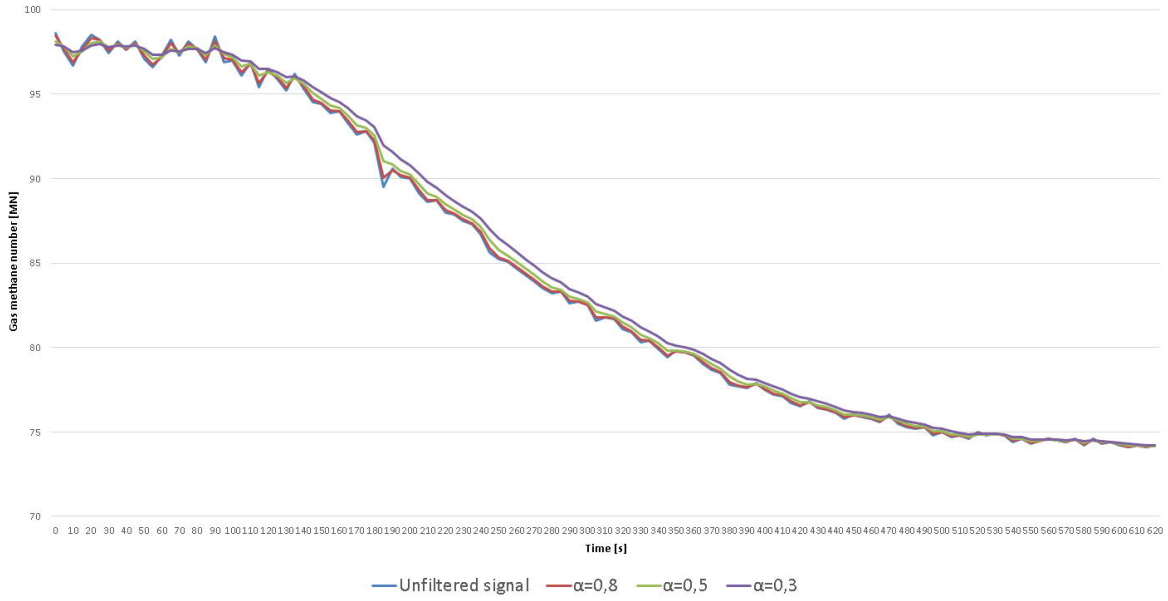

Figure 30. Signal filtration with an exponential smoothing filter.

A better smoothing effect is achieved with a smaller value on the smoothing factor α, but a smaller smoothing factor will also result in a larger phase shift between the input and output signals.

7.3.4 Filter recommendation

When comparing these three different filters, it can be concluded that the exponential smoothing filter is the best solution for this control function. The advantage of this filter is its wide usage area in different applications and that the level of smoothing can be adjusted by changing one parameter. The following values of smoothing factor α are recommended to be used in this application.

Table 1. Recommended filter settings.

Smoothing factor α	Level of filtration
1	No filtation
0.5	Light filtration
0.3	Heavy filtration

For most installation a smoothing factor (α) of 0,5 is recommended, but if more filtration of the input signal is needed a lower smoothing factor can be used. However, this filter will be designed for a measurement equipment with a sampling rate of 0,2 Hz and will only work properly together with this kind of measurement equipment. Modification must be done to

the filter design, if the filter is going to be used for some other measurement equipment with a different sampling rate. The filter will be designed with a model in Simulink and this filter model is then converted to ST code for implementation into the PLC system. The following figure illustrates the Simulink model of the exponential smoothing filter.

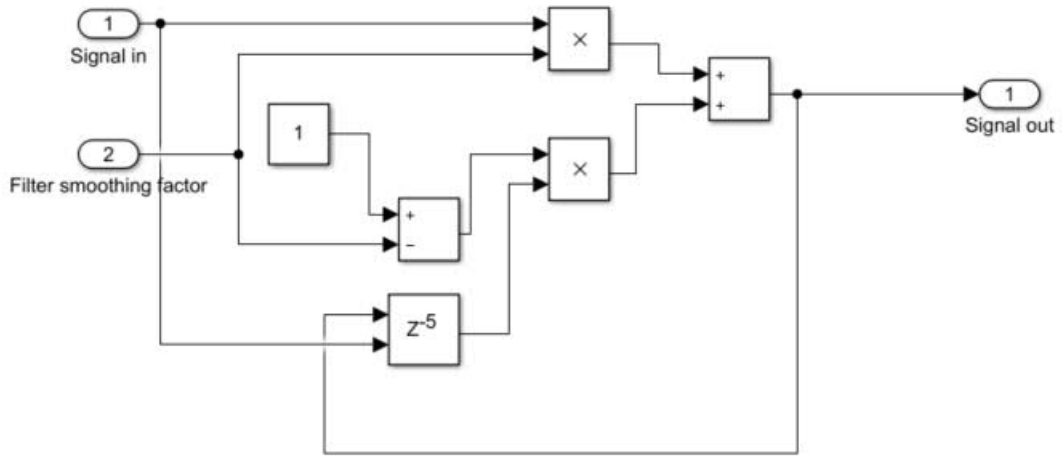

Figure 31. Simulink model of the exponential smoothing filter.

The Simulink PLC coder uses the filter model to generate the corresponding ST code and the generated code for this filter model is 55 code lines and part of the code is presented below.

Code example 1. Part of generated ST code for filter model.

```
IF need_init THEN
  (* InitializeConditions for Delay: '&lt;S1&gt;/Delay4' *)
  icLoad := 1;
  need_init := FALSE;
END_IF;
(* Delay: '&lt;S1&gt;/Delay4' *)
IF icLoad &lt;&gt; 0 THEN
  FOR i := 0 TO 4 DO
    Delay4_DSTATE[i] := In1;
  END_FOR;
END_IF;
```

This code can then be imported to the PLC system, either by creating an FBD-block containing the code or if the whole PLC program is programmed in ST code, the filter part of code is just added to the existing code.

7.4 Inputs, output and parameters of MN_derating controller

The MN_derating controller have some parameters that needs to be configured, to ensure proper function of the controller. All needed inputs, outputs and parameter signals are presented in the following table.

Table 2: List and description of the MN_derating controller variables.

I/O parameters	Parameter	Data type	Description
Parameters	Design_power	REAL	Design power output of engine, project specified or stated in the performance manual
	Design_MN	REAL	Design gas methane number, project specified or stated in the performance manual (serves as breakpoint in Kknock curve)
	X-axis_MN_derating_curve	REAL	Chosen MN point in Kknock curve
	Y-axis_derating_factor	REAL	Derating factor from Kknock curve at chosen MN point
	Deadband	REAL	Deadband setting, specified in amount MN
	Rising_rate_limit	REAL	Measured_MN signal rising rate changes no faster than the specified limit given in load%/min
	Filter_smoothing_factor	REAL	Value of filter smoothing factor α, between 0 and 1. A larger value reduces the level of smoothing and no filtration with α = 1
Inputs	Measured_MN	DINT	Measured methane number of gas used as fuel in MN*100
	Delay_time	DINT	Delay the output signal with specified time in seconds
	Disable	BOOL	When input is active, MN_derating controller is disabled and output is 0
Output	MN_derating_offset	DINT	Amount of needed engine deration in kW*10

The gas analyzer sends the gas mixture concentration over the MODBUS TCP/IP protocol to the PLC system. This data is then used by the methane number calculator, which is calculating the corresponding methane number for the provided concentration. This calculated value is used by the MN_derating controller and it controls the maximum allowed engine power output dependent on the provided methane number value. The output from MN_derating controller is in amount of kW that the engine power should be reduced from the design power parameter. This value is sent to the maximum output limiter, this controller takes also in to consideration the other two derating factors, these are the K_{TC} derating factor and K_{GA} derating factor. Maximum allowed engine power output is decided from the lowest value of these three derating functions and this value is sent over MODBUS TCP/IP protocol to the engine control unit (ECU). The following figure illustrates the communication between the gas analyzer, PLC and ECU.

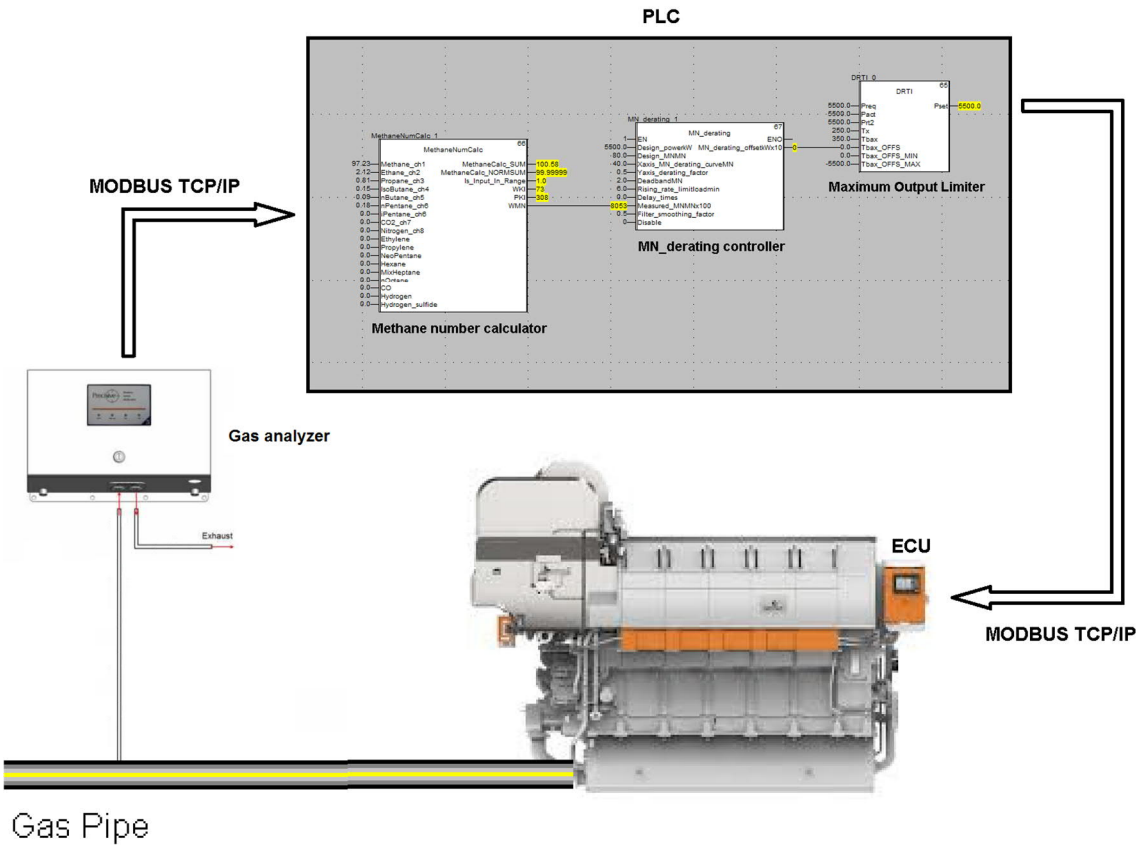

Figure 32. Layout for communication between gas analyzer, PLC and ECU.

7.5 Deadband

The owner of the powerplant and parties responsible for the electrical grid sometime desire to have as stable power output as possible to the electrical grid. This can be achieved with implementation of a deadband function in the controller, so that the load reduction can be done in steps to avoid continuous power fluctuations. The deadband setting is specified in MN units and the following figure illustrates the effect of different settings.

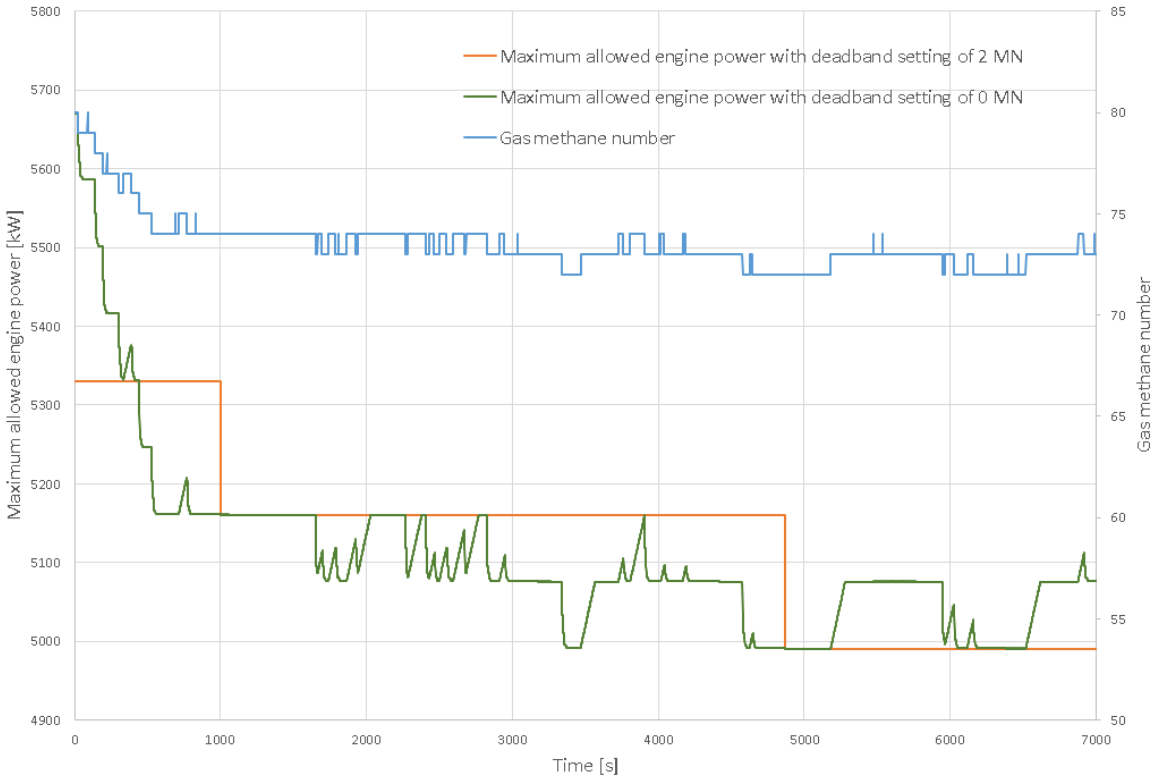

Figure 33. Influence of deadband setting.

The deadband setting is fully adjustable, but in most cases a deadband setting of 2 MN units is recommended for avoiding continuous power fluctuations, but still maintaining a fast response.

7.6 Output delay

The installation location of the gas analyzer will affect how long time it takes for the gas that have been analyzed until it reaches the engine. A long distance between the analyzing point and the engine can result in a significant time delay and it might be desirable that the controller's output signal is not immediately changed. The delay functionality is used to delay changes of the output signal with the corresponding time. This delay time originates not only from the time it takes for the gas to flow through the piping system, but also from the response time of the used measurement equipment. Both these two will have an impact and need to be considered to obtain the combined delay time of the complete system.

7.6.1 Gas analyzer response time

The response time of the gas analyzer comes from the transportation delay, which is the time it takes for the gas mixture to reach the analyzer and then the exchange rate in the measurement cell of the sensor. Maximum allowed flow to the gas analyzer is 15 litres per minute (LPM), but the supplier recommends a constant gas flow of one LPM and a flow regulator is used to achieve this. The sample inlet pipe is a ¼ inch 316 stainless steel pipe and it is recommended that the outlet pipe should be of a bigger diameter than the inlet to assure safe and unforced flow of the gas through the analyzer. It is also recommended that the sample line should be as short as possible, and a sample line longer than 5 meters needs a bypass sweep to reduce the transportation delay time. The following table contains information given by the manufacturer about the measurement cell exchange rate.

Table 3. Gas cell exchange rate in seconds dependent on flow rate.

	T90	T95	T99
0.5 SLM	25	35	60
1 SLM	20	25	40
5 SLM	4	5	6

In this table the T90 denotes that all the gas mixture in the measurement cell has been exchanged with 90 percent certainty, T95 with 95 percent certainty and T99 with 99 percent certainty.

Two response tests were conducted to verify these values, it was decided to do the test with two flow settings, 0,5 and 1 litre per minute. The tests were conducted by first supplying the gas analyzer with pure nitrogen. The gas analyzer is then supplied with LNG instead of nitrogen by actuating a valve. The time that it takes until the gas analyzer gives the correct concentration readings is recorded. The following figures illustrates the result from these gas analyzer response tests.

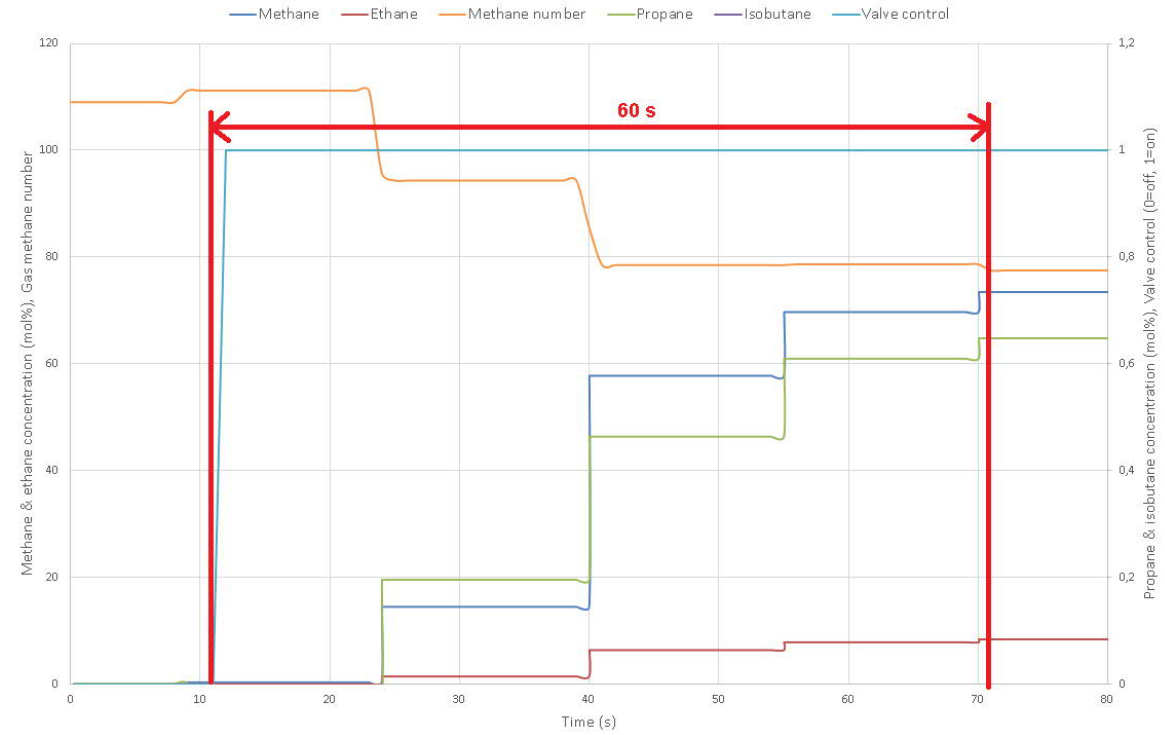

Figure 34. Gas analyzer response test with a gas flow of 0,5 litre per minute.

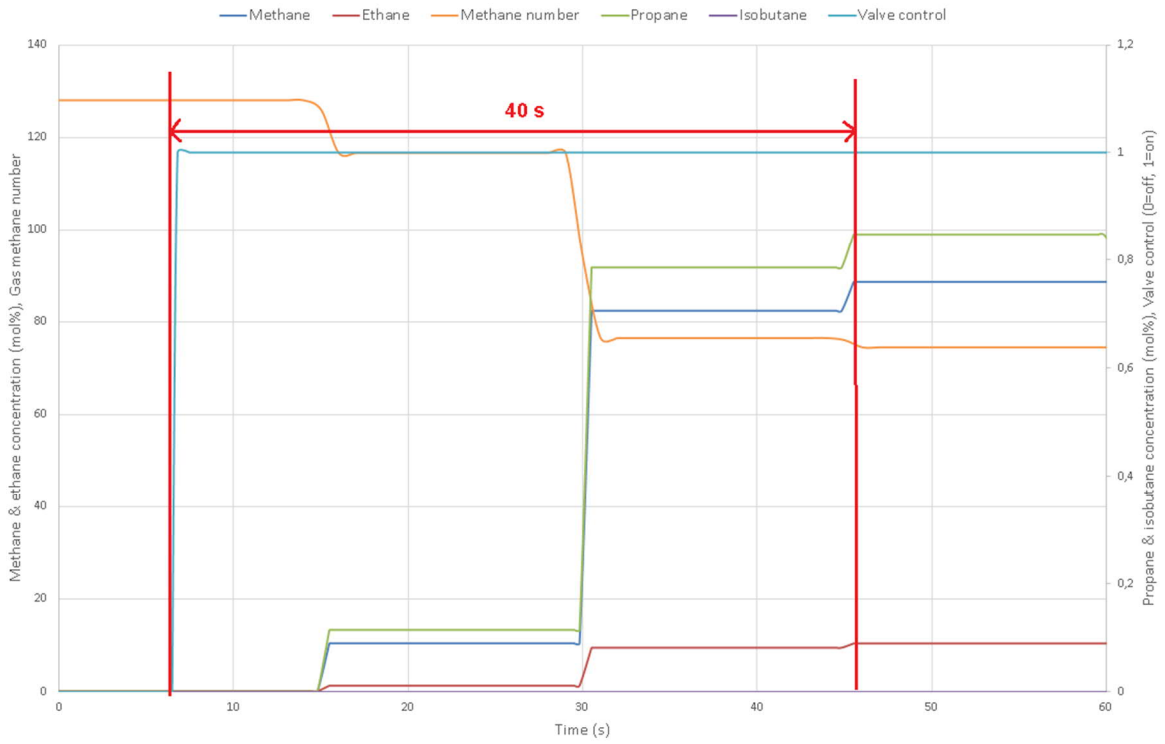

Figure 35. Gas analyzer response test with a gas flow of 1 litre per minute.

From these two gas analyzer response tests, it can be concluded that values given by the manufacturer correspond to the real response time, since the T99 values and the measured values are identical. During normal operation when using the gas analyzer for continuous measurement, it will most of time give a correct reading even that not all the gas mixture has been exchanged and therefore the T90 exchange rate value is used for response time calculation. In addition to this there are also some additional delays due to the analyzing process and data processing. Calculation of the complete response time for the gas analyzer is presented in the following figure.

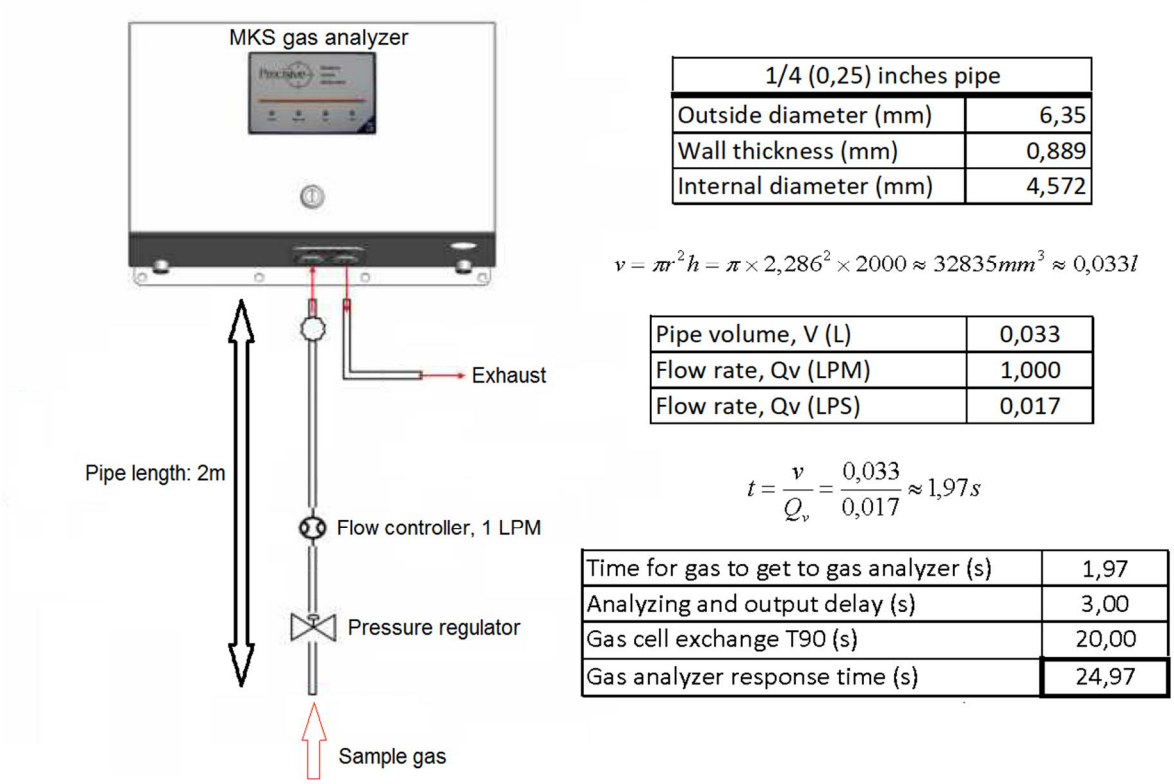

1/4 (0,25) inches pipe	
Outside diameter (mm)	6,35
Wall thickness (mm)	0,889
Internal diameter (mm)	4,572

$$v = \pi r^2 h = \pi \times 2{,}286^2 \times 2000 \approx 32835 mm^3 \approx 0{,}033 l$$

Pipe volume, V (L)	0,033
Flow rate, Qv (LPM)	1,000
Flow rate, Qv (LPS)	0,017

$$t = \frac{v}{Q_v} = \frac{0{,}033}{0{,}017} \approx 1{,}97 s$$

Time for gas to get to gas analyzer (s)	1,97
Analyzing and output delay (s)	3,00
Gas cell exchange T90 (s)	20,00
Gas analyzer response time (s)	24,97

Figure 36. Gas analyzer response time calculation.

Total response time for this example installation with two meters pipe length to the gas analyzer is about 25 seconds, where the largest part comes from the delay time originating from the measurement cell exchange rate.

7.6.2 Transportation delay in gas piping system

The transportation delay time in gas piping system can be calculated from the pipe volume. Since consumption measurements are often done on mass flow basis, it needs to be converted to volume flow by calculating the gas density with the ideal gas law, that is defined by the following equation:

$$Pv = nRT \tag{11}$$

In this equation P stands for pressure, v stands for volume, n is the number of moles, R is a gas constant and T is the temperature. The ideal gas law equation can be rewritten, since the number of moles can be defined as mass divided by molecular weight and this gives the following equation:

$$Pv = \left(\frac{m}{M}\right)RT \tag{12}$$

In this equation m is the mass and M stands for molecular weight. Since density equals mass over volume, which gives that density can be calculated with the following equation:

$$\rho = \frac{PM}{RT} \tag{13}$$

The volume flow can be calculated when the density for the gas mixture is known. The time it takes for gas mixture to reach the engine is then calculated by dividing the volume flow with the volume of the gas pipes according to the following equation:

$$t = \frac{v}{Q_v} \tag{14}$$

7.6.3 Example of delay

A calculation example for a gas pipe system illustrated in the following figure with DN100 pipes are available in appendix 2.

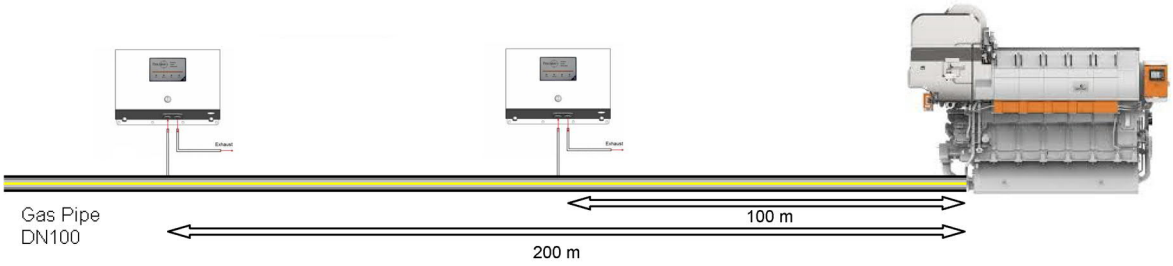

Figure 37. The transport delay is dependent on the measurement location.

This example demonstrates the difference between 100 and 200 meters distance between the gas analyzer sampling point and engine. The transport delay time calculations are done with three different gas pressures, they are 4, 8 and 11 bars. These calculations are calculated with an engine, that have a power output of 6000 kW, fuel consumption varies a little bit dependent on the energy content of the used gas, but for this example a gas mixture with LHV of 34 MJ/Nm^3 is used and this gives a fuel consumption of approximately 900 kg/h. The following table presents the result from the transport delay calculations in appendix 2 with the combined delay time of both the incoming gas pipe transport delay and the gas analyzer response time.

Table 4. Combined delay time for an engine with a fuel consumption of 900 kg/h.

Pipe length and pressure (gauge bar)	Transport delay in gas piping system (s)	Gas analyzer response time (s)	Combined delay time (s)
100 m with 4 bar	12,6	25,0	-12,3
100 m with 8 bar	22,7	25,0	-2,3
100 m with 11 bar	30,3	25,0	5,3
200 m with 4 bar	25,3	25,0	0,3
200 m with 8 bar	45,4	25,0	20,4
200 m with 11 bar	60,5	25,0	35,6

The gas analyzer response time is constant since the flow regulator gives a constant gas flow of one LPM to the gas analyzer. Combined delay time values in red, indicates that the gas will reach the engine with 90 percent certainty before it has been analyzed by the gas analyzer.

Based on this result it is not recommended to place the gas analyzer sampling point closer than 100 meters before the gas regulator unit. If the sampling point is placed closer, it is resulting in that the gaseous fuel is not being analyzed before it is used by the engine and therefore the control system cannot react in time to take appropriate control action. A longer reaction time to react on variations in the incoming gaseous fuel can be achieved, by using

a higher pressure in the incoming gas pipe. The following figure illustrates the recommended sampling location for a power plant consisting of two engines.

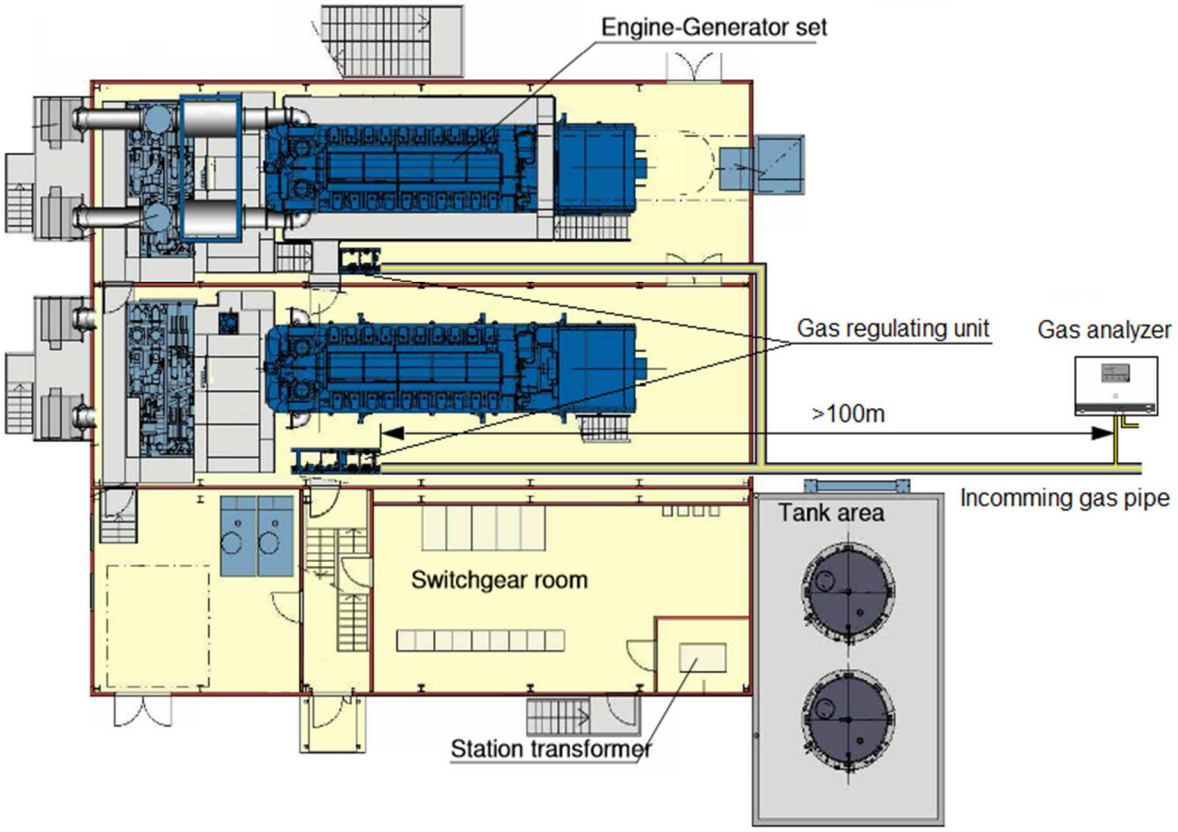

Figure 38. Recommended sampling location for a power plant consisting of two engines.

The required distance between the gas regulating unit and sampling point of the gas analyzer can vary between different power plants and it is based on number of engines in the power plant, the total fuel consumption of all engines, gas pressure in the incoming pipe and the size of the incoming gas pipe.

8 Simulation and testing

A simulation of the MN_derating controller behaviour has been done with logged measurement data from Toftlund Fjernvarme, located in Denmark. Toftlund Fjernvarme is a combined heat and power (CHP) plant that produces district heating for the nearby community and the produced electricity is feed to the national electrical grid. The engine heats up a water reservoir, so the normal running profile for this power plant is that they run their W18V34SG engine on full load until the water reservoir is heated up and then the engine is shut down until more heating is needed.

There is an MKS Precisive gas analyzer installed on the incoming gas pipe to the power plant. This gas analyzer is used to measure the gas composition of the incoming gaseous fuel mixture. The measured gas composition is then used to calculate MN and LHV of the gaseous fuel. The following figure illustrates the communication layout used for the simulation process of the MN_derating controller behaviour.

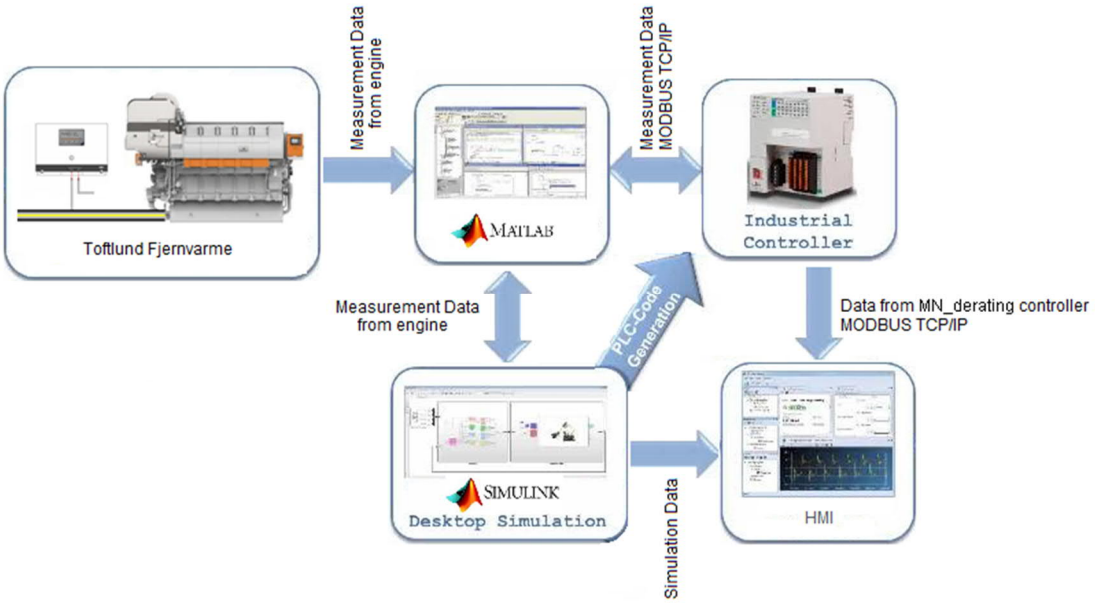

Figure 39. Communication layout for the simulation process.

The simulation process is accomplished by that measurement data from Toftlund Fjernvarme is imported to Matlab where it can be accessed and used by the MN_derating controller model in Simulink. Simulation and testing of the model are done with this data and code generation is done after correct function is verified. This generated ST code of the MN_derating controller is then implemented into a PLC system. The following figure illustrates a simulation done by using data from Toftlund Fjernvarme.

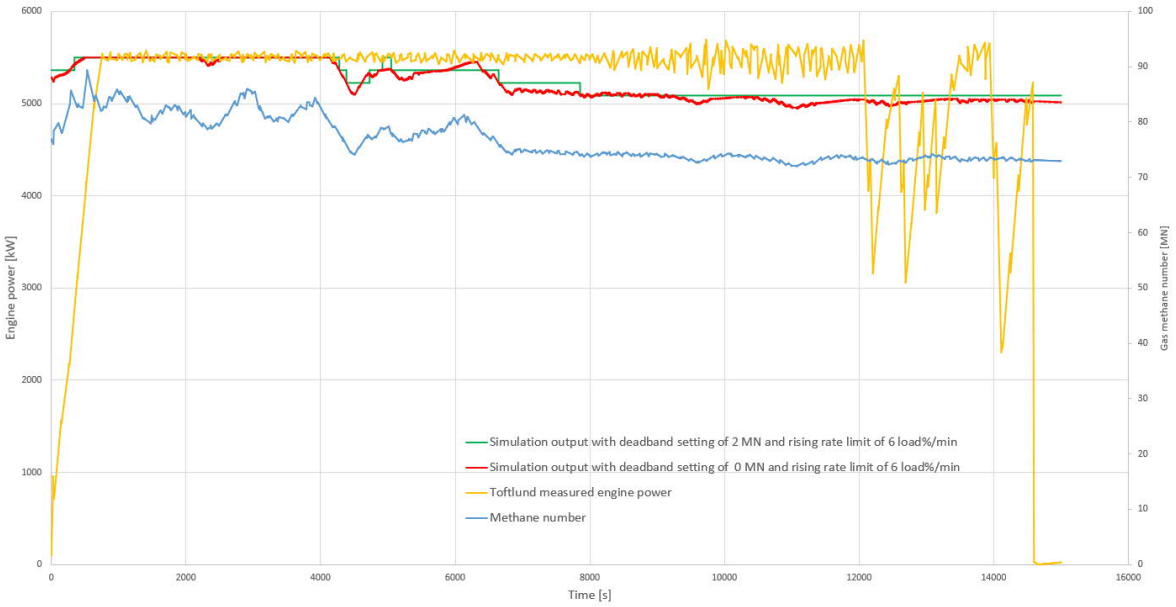

Figure 40. Simulation of the MN_derating controller.

This simulation is done with a maximum engine power output of 5500 kW, the methane number breakpoint is 80 MN and after that the derating factor is 0,0125, which is resulting in 68,75 kW power reduction per MN. From the previous figure it can be seen that the power output that is represented by the yellow line starts to fluctuate after 10000 seconds. This indicates engine knock and eventually the engine even had to be stopped. The engine was operating at a higher power output than what the MN_derating controller would have allowed, so If the MN_derating controller would have been used both the engine knock and the unnecessary engine stop could possibly have been avoided. This simulation verifies correct function of the controller model in Simulink and ST code can be generated for implementation into a PLC system.

The generated ST code for the MN_derating controller can then be implemented into a PLC system. Testing of the controller in the PLC environment are done with the same measurement data used for the controller model simulation in Simulink. This is achieved by using a Matlab script, that is sending the data to the PLC system over the MODBUS TCP/IP protocol. This script is presented below:

Code example 2. Matlab script for sending data over MODBUS TCP/IP.

```
m = modbus('tcpip', '192.168.8.77', 502) %IP address of PLC system
ind = 1;
load Data %Load measured data from Toftlund Fjernvarme
```

```
x=0;
for ind = 1:6001
  x= Data(ind); %Data one sample at time
  write(m,'holdingregs',1,[x 2]) %write MN to address 40001 & status to
40002
  pause(5) %0,2 Hz send frequency
end
write(m,'holdingregs',2,0)%write status address back to 0
```

A comparison has been done between the behaviour of the controller in Simulink and PLC system. The maximum allowed engine power output from the PLC controller and the maximum allowed engine power output coming from the simulation of the model in Simulink are presented in the following figure.

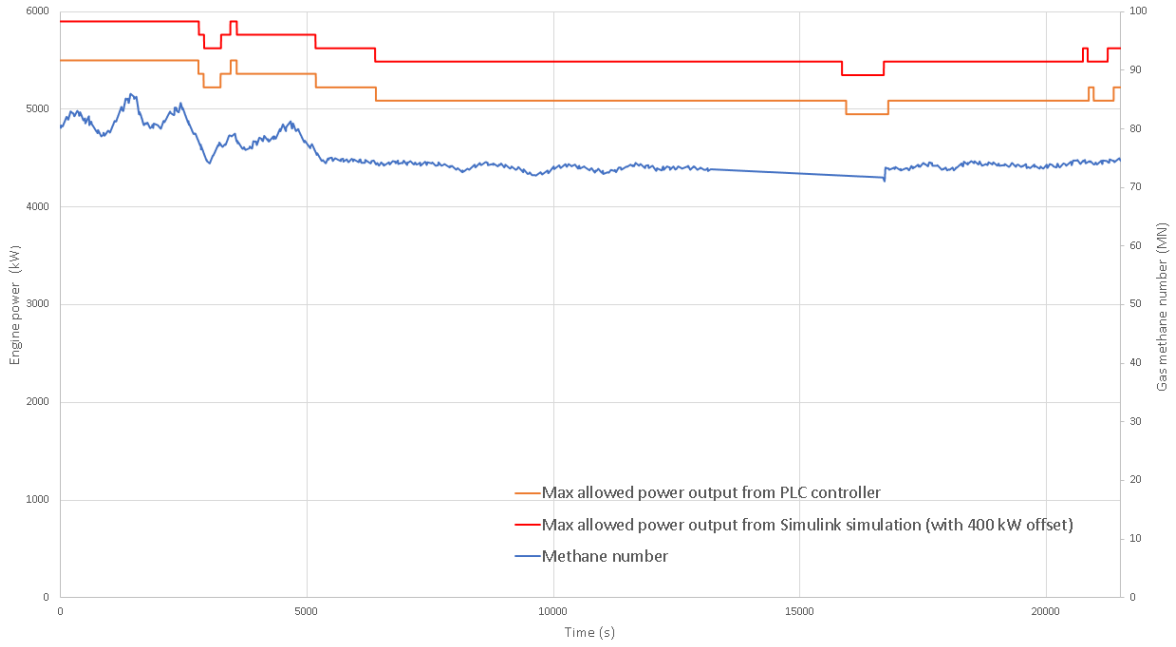

Figure 41. Comparison between data from the Simulink simulation and output from the PLC controller.

In this figure the maximum allowed power output simulated by the controller model has an offset of 400 kW, so that the lines are not on top of each other. In Figure 41 it is shown that both the data coming from model simulation and the data coming from the real controller in the PLC system are identical and this confirms correct behaviour of the controller in the PLC system.

9 Alternative engine control strategies

A part of this thesis work is to investigate other control strategies that could be used to minimize derating of gas engines and maximize the energy production. This investigation is done only as a literature review and could function as a starting point for future engine testing.

One method of avoiding engine derating when operating on a gaseous fuel with lower methane number is to compensate with a leaner air-fuel mixture, by increasing the charge air pressure. A leaner air-fuel mixture will move further away from the knock region in the operating window and closer to the misfire region. This allows that the engine still can maintain a high power output using a gaseous fuel with less knock resistance. This can be done as an open loop control with a control map depending on BMEP and MN. The following table illustrate an example of how many bars the charge air pressure could be increased with falling MN.

Table 5. Increasing of charge air pressure dependent on BMEP and MN.

MN / BMEP	55	60	65	70	75	80	90
15	0,2	0,2	0,1	0,1	0,1	0	0
17	0,2	0,2	0,2	0,2	0,1	0	0
21	0,2	0,2	0,2	0,2	0,1	0	0
23	0,3	0,2	0,1	0,1	0,1	0	0
25	0,4	0,3	0,2	0,1	0,1	0	0
27	0,4	0,4	0,3	0,2	0,1	0	0
30	0,5	0,4	0,3	0,2	0,1	0	0

Increasing the charge air pressure will result in a slower combustion and higher pumping work done by the piston and therefore the efficiency of the engine will be lower (Porpatham, Ramesh & Nagalingam 2008, pp. 1651–1659). The leaner air-fuel mixture will also affect exhaust gas emissions mainly by that the nitrogen oxide (NOx) emission will decrease and hydrocarbon (HC) emission will increase (Gupta 2013, pp. 171-183). Therefore, engine type specific testing must be done to find proper values for the control map.

The charge air temperature will also affect the knock tendency of the engine, since a lower temperature on the charge air supplied to the engine can improve the knock limits by moving away from the knock region in the operating window (Haghgooie 1990).

An increase in the charge air temperature will result in an increase in the inlet temperature of the air-fuel mixture supplied to the engine and that increases the temperature at the end of compression, which in turn increases the temperature of the combustion, thus shortening the delay period and greatly increasing the tendency to knock (Gupta 2013, pp. 171-183). Most turbocharged engines have a charge air cooler that reduces the temperature of the charge air before it is supplied to the engine. This makes it possible to compensate for a gaseous fuel with a higher knock tendency by lowering the charge air temperature. However, the amount of cooling of the charge air that can be achieved is often limited to the ambient condition of the location where the engine is operated and therefore the possible reducing effect of the knock tendency is limited.

Second method to avoid derating is by controlling the ignition timing. The start of combustion can be controlled with the ignition timing parameter and this affects the combustion pressure (Gupta 2013, pp. 171-183) (Mittal, Revier & Heywood 2007). The ignition timing parameter needs to be dependent on BMEP and MN and an example of possible settings can be found in the following table.

Table 6. Ignition timing dependent on BMEP and MN.

MN / BMEP	55	60	65	70	75	80	90
15	14°	13°	17°	17°	17°	17°	17°
17	14°	14°	14°	19°	19°	19°	19°
21	14°	17°	17°	17°	19°	19°	19°
23	12°	13°	13°	17°	17°	18°	19°
25	13°	13°	13°	17°	17°	18°	18°
27	8°	10°	12°	13°	15°	18°	18°
30	8°	10°	12°	13°	15°	18°	18°

In this table the ignition timing is given in crank angle degrees before top dead centre and the ignition timing is retarded with falling MN, so that the ignition happens later. This results in a lower combustion pressure inside the combustion chamber, which will give a better knock resistance, because autoignition of the end gas is strongly dependent on pressure and temperature inside the combustion chamber (Joshi 2017, p. 21). Since controlling the ignition timing will affect both the efficiency and the exhaust gas emissions of the engine, specific engine type testing needs to be done in order to find proper values for the control map.

Third method of avoiding engine derating when operating on a gaseous fuel with lower methane number is to use exhaust gas re-circulation (EGR). This is an effective technique to reduce knock especially if the exhaust gas is cooled before it is re-circulated into the combustion chamber. This technique is used e.g. in modern gasoline engines and will also work in gaseous fuel engines, since the knocking tendency reducing effect comes from that the cooled exhaust gas has already burnt and therefore cannot undergo combustion again (Hoepke, Jannsen, Kasseris & Cheng 2012, pp. 547-559). The cooled exhaust gas soaks up the heat from the compressed air-fuel mixture, which reduces the combustion temperature and often also enhances the flame propagation speed (Szybist, Wagnon, Splitter & Pitz 2017, pp. 2305-2318). EGR is an effective technique in reducing the knocking tendency of engines, since it is resulting in a reduction in combustion temperature and increase in flame propagation speed (Joshi 2017, p. 21). Specific engine type testing needs to be done to determine the amount of needed EGR with different gaseous fuels. Some additional engine components are also needed to realize this method.

A combination of the two first mention methods would preferably be the best solution. A combined effect for better resistance against knock will be achieved by both increasing the charge air pressure and changing the ignition timing. The advantages with these methods are that they can be accomplished with no additional engine components.

10 Conclusion and future development

In the following chapters the result of the thesis work will be summarised and there will be a discussion about future development of the engine control possibilities using the gaseous fuel quality determination concept. Advantages and disadvantages of the model-based design approach for PLC programming will also be discussed.

10.1 Conclusion

The objective of this thesis work was to design and implement a controller that is determining maximum allowed engine power output based on the gaseous fuel quality. A model-based design is used and this makes it possible to implement the controller using numerous PLC models from different manufactories. The controller has functions that fulfils all requirements from the requirements specification and functionality tests of the controller has been validated with simulations that uses measured data from an operating power plant. In addition to simulations, there have also been system tests of the controller performed in the PLC environment to ensure correct functionality in this environment. Next step is to implement the controller to a pilot installation, e.g. a power plant with a couple of engines. This pilot installation will give feedback about the controller's functionality and to identify and solve potential issues. After it has been verified that the controller is functioning correctly, it can be released and taken into use on all powerplant installations that has a gas quality measurement device.

A brief literature review was also conducted to investigate some alternative control strategies that use the gas quality measurement technology. These control strategies could be used as an alternative to engine derating in order to avoid engine knock. The outcome of the literature review is that a combination of both increasing the charge air pressure and controlling the ignition timing would preferably be the best solution for achieving a better resistance against knock when operating engines on gaseous fuels with low methane number. The final course of action to protect the engine from damage, if the alternative control methods has not sufficient effect to avoid engine knock will always be to reduce the power output.

Wärtsilä will start to recommend the usage of a gaseous fuel quality measurement device for their costumers and the goal is that all future power plant installations will have one installed. Some of the benefits of using the gas quality measurement technology are that the performance of the engine can be optimized, which results in lower fuel consumption. By using the MN_derating controller the protection against engine knock is enhanced, which results in a safer operation of the engine and improves the reliability.

10.2 Future development

Future research needs to be done on the alternative control strategies and how they could be realised. At the time of writing most of the functions that are connected to the engine operation itself are controlled by the engine control unit, while the safety functions like the MN_derating controller are controlled by the PLC system. To get a good working interaction between the alternative control strategies and the derating controller an investigation about the communication between these needs to be done.

10.3 Discussion about model-based design for PLC programming

There are several benefits of using a model-based design approach for programming PLC systems. Some of the benefits are that it helps to manage complex systems and the ability to run simulations against a plant model. This enables debug possibilities of the control model and that is resulting in a better verification of the function and that design problems and uncertainties can be solved in an early stage of the development process. The biggest advantage of using a model-based design approach is the possibility for code generation to both C, C++ and structured text code, this enables that the same model can be used and implemented to both PLC systems and other control systems. The generated structured text code enables multiple PLC platform support and therefore it can be used in numerous PLC models from different manufactories.

The model-based design approach for programming is still new in the PLC field and this leads to several disadvantages. One of the biggest disadvantages is that there is still a limitation in supported functions. At the time of writing, e.g. Simulink PLC coder only supports a few blocks of all available blocks in Simulink and this can be a limitation in achieving correct function. Another disadvantage is the troubleshooting, this is more connected to the structured text programming language and not with the model-based design itself. The troubleshooting of the structured text code can be more complicated than

graphics-based PLC programming languages, since the text environment often feels somewhat unfamiliar compared to graphics-based methods.

Even that the model-based design approach for PLC programming is still under development, it is continuously gaining more interest and it will most likely have a major role in how future PLC programming is done, since it has the benefits of simulation possibilities and the possibility for rapid prototyping.

11 Refereces

Aarenstrup, R., 2015. *Managing Model-Based Design.* MathWorks, Inc, Natick.

Andersen, P., 1999. *Algorithm for methane number determination for natural gases.* Danish Gas Technology Centre a/s, Hørsholm.

Bui, Y., 2011. *Consequences of technology choices DF or SG.* Wärtsilä

Brown, R., 1963. *Smoothing Forecasting and Prediction of Discrete Time Series.* Englewood Cliffs, NJ: Prentice-Hall.

CIMAC, 2015. *Impact of Gas Quality on Gas Engine Performance.* [Online] Available from:https://www.cimac.com/cms/upload/workinggroups/WG17/CIMAC_WG17_Position_Paper_Impact_Gas_Quality_on_Gas_Engine_Performance_2015_Jul.pdf [Accessed 02.04.2019], CIMAC Position Paper.

Demirbas, A., 2010. *Methane Gas Hydrate.* Springer, London

Fallah, S., Khajepour, A., & Goodarzi, A., 2016. *Electric and Hybrid Vehicles - Technologies, Modeling and Control: A Mechatronic Approach.* John Wiley & Sons, Ltd.

Grönroos, J., 2016. *Online gas quality measurement and engine control.* Helsinki: Aalto University.

Gupta, H., 2013. *Fundamentals of internal combustion engines.* PHI Private Ltd.

Haghgooie, M., 1990, *Effects of Fuel Octane Number and Inlet Air Temperature on Knock Characteristics of a Single Cylinder Engine.* SAE Technical Paper 902134, 1990.

Hoepke, B., Jannsen, S., Kasseris, E., Cheng, W., 2012. *EGR Effects on Boosted SI Engine Operation and Knock Integral Correlation.* SAE Int. J. Engines 5(2), 2012.

Heywood, J. B., 1988. *Internal Combustion Engine Fundamentals. McGraw-Hill series in mechanical engineering.* McGraw-Hill, New York.

Högberg, D., 2018. *Measures to utilize real-time gas quality analyses for engine control.* Turku: Åbo Akademi University

Joshi, A. S., 2017. *Effect of spark advance and fuel on knocking tendency of spark ignited engine.* Michigan Technological University.

Leiker M, Christoph K, Rankl M, Cantellieri W, Pfeifer U. (AVL, Graz, Austria), 1972. *Evaluation of anti-knocking property of gaseous fuels by means of methane number and its practical application to gas engines.* ASME-72-DGP-4.

Malenshek M. & Olsen D. B., 2008. *Methane number testing of alternative gaseous fuels.* Fort Collins: Colorado State University

Porpatham, E., Ramesh, A., Nagalingam, B., 2008. *Investigation on the effect of concentration of methane in biogas when used as a fuel for a spark ignition engine.* Fuel 87, 1651–1659.

Pulkrabek, W., 2004. *Engineering Fundamentals of the Internal Combustion Engine. Prentice Hall*

Robertson, S., Robertson, J., 2012. *Mastering the Requirements Process: Getting Requirements Right.* Addison-Wesley Professional.

Smith, S., 1999. *The Scientist and Engineer's Guide to Digital Signal Processing, Second Edition.* California Technical Publishing, San Diego.

Szybist, J., Wagnon, S., Splitter, D., Pitz, W. et al., 2017. *The Reduced Effectiveness of EGR to Mitigate Knock at High Loads in Boosted SI Engines.* SAE Int. J. Engines 10(5):2017

Mittal, V., Revier, B., Heywood, J., 2007. *Phenomena that Determine Knock Onset in Spark-Ignition Engines.* SAE Technical Paper 2007-01-0007, 2007.

MKS Instruments, n.d. a. *Precisive 5 Hydrocarbon Composition Analyzer.* [Online] Available from: https://www.mksinst.com/f/precisive-5-hydrocarbon-composition-analyzer [Accessed 17.02.2019].

MKS Instruments, n.d. b. *Precisive UV-IR Platforms.* [Online] Available from: https://www.mksinst.com/docs/UR/PrecisiveUV-IRPlatforms.aspx [Accessed 17.02.2019].

van Essen, M., & Gersen, S., 2015. *Next generation knock characterization.* DNV GL, Groningen.

van Essen, M., & Gersen, S., 2018. *Oil and gas workshop, part 2: Modelling the W34SG engine*. [Lecture] Wärtsilä Land and Sea Academy Vaasa, 15th February 2018.

Wärtsilä, 2009. *WÄRTSILÄ 50DF ENGINE TECHNOLOGY*. [Online] Available from: http://cdn.wartsila.com/docs/default-source/Power-Plants-documents/w%C3%A4rtsil%C3%A4-50df.pdf [Accessed 02.04.2019].

Wärtsilä, 2015. *Performance Manual Wärtsilä 34SGC*.

Wärtsilä, 2018. *Wärtsilä 50DF product guide*. [Online] Available from: https://cdn.wartsila.com/docs/default-source/product-files/engines/df-engine/product-guide-o-e-w50df.pdf?sfvrsn=9 [Accessed 02.04.2019].

LIST OF APPENDICES

Requirements specification.

Specification	Required or Optional	Value of importance (1-5)	Final Acceptance Test or Method	Customer Approved
Multi PLC type support from different manufacturers	Required	5	System test	Yes
User-friendly commissioning	Required	4	System test	No
Easy parameterization	Required	3	System test	Yes
Interaction with other control functions	Required	5	System test	Yes
Adjustable derating factor	Required	5	Simulation & system test	Yes
Input signal filtering	Required	5	Simulation & system test	Yes
Adjustable level of filtering	Required	3	Simulation & system test	Yes
Different ramp rates for rising and falling MN	Required	4	Simulation & system test	Yes
Adjustable ramp rate for rising MN	Optional	3	Simulation & system test	Yes
Fast response for falling MN	Required	5	Simulation & system test	Yes
Deadband control	Required	4	Simulation & system test	Yes
Output delay	Optional	2	Simulation & system test	Yes
Fault mode	Optional	2	System test	No
Functionality test, fault testing (Bug testing)	Required	5	Simulation & system test	Yes
User documentation	Required	2	System test	Yes
After release updates	Required	4	Service department	Yes

Transport delay time calculation.

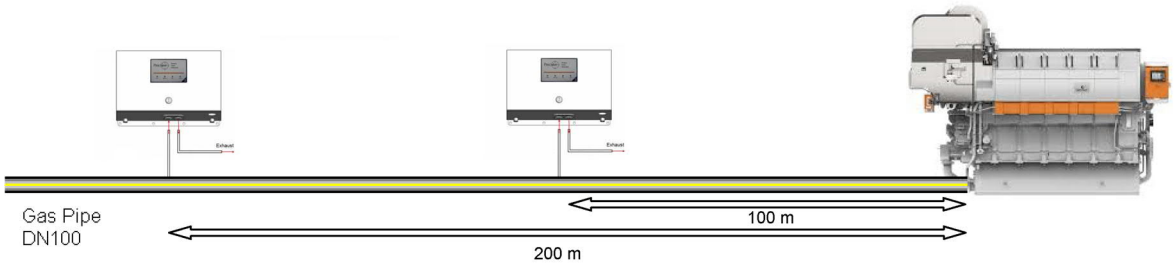

Figure 1. Gas analyzer sample locations.

Molar mass of pure methane is 16,043 g/mol, normally molar mass of natural gas is in the range between 16 to 19 g/mol. Average molar mass from fuel samples taken at Wärtsilä's engine laboratory in Vaasa gives 17,29 g/mol.

Table 1. Values used for density calculations.

Symbol	Description	
T	Temperature (K)	293
	Ambient Pressure (Pa)	101300
M	Average molar mass (kg/mol)	0,01729
R	Gas constant (J/mole Kelvin)	8,3145
	Gas pressure in pipe (gbar)	4, 8 & 11
P	Gas absolute pressure in pipe (Pa)	501300 901300 1201300

Equation for density: $$\rho = \frac{PM}{RT} \quad (1)$$

Table 2. Density calculation results.

Gas pressure in pipe (gauge bar)	Gas density (kg/m3)
4	3,558
8	6,397
11	8,526

Table 3. Pipe measurements.

DN 100 pipe	
Outside diameter (mm)	114,3
Wall thickness (mm)	4
Internal diameter (mm)	106,3
Pipe lenght (mm)	100000
	200000

Equation for volume:

$$V = \pi r^2 h = \pi \times 53{,}15^2 \times 100000 \approx 887475577{,}3\ mm^3 = 0{,}8875\ m^3 \quad (2)$$

$$V = \pi r^2 h = \pi \times 53{,}15^2 \times 200000 \approx 1774951154{,}6\ mm^3 = 1{,}7750\ m^3 \quad (3)$$

Table 4. Pipe volume (V) calculation results.

Pipe length (m)	Pipe volume (m3)
100	0,8875
200	1,7750

Equation for volume flow: $Q_V = \frac{Q_m}{\rho}$ (4)

Table 5. Results for gas volume flow (Q_V) calculation from a gas mass flow (Q_M) of 900 kg/h

Gas pressure in pipe (gauge bar)	Gas density (kg/m3)	Gas Volume flow (m3/h)
4	3,558	252,961
8	6,397	140,696
11	8,526	105,560

Equation for delay time: $t = \frac{V}{Q_V}$ (5)

Table 6. Transport delay time for an engine with a fuel consumption of 900 kg/h.

Pipe length and pressure (gauge bar)	Transport delay in gas piping system (s)
100 m with 4 bar	12,6
100 m with 8 bar	22,7
100 m with 11 bar	30,3
200 m with 4 bar	25,3
200 m with 8 bar	45,4
200 m with 11 bar	60,5